









ORIGINAL RESEARCH

Novel Mechanism of Microvesicle Regulation by the Antiviral Protein Tetherin During HIV Infection

Emily A. Weber , PhD; Meera V. Singh , PhD; Vir B. Singh , PhD; Joseph W. Jackson , PhD; Sara K. Ture , BS; Sumanun Suwannakorn , PhD; Craig N. Morrell , PhD; Sanjay B. Maggirwar , PhD

BACKGROUND: Microvesicles are cell membrane–derived vesicles that have been shown to augment inflammation. Specifically, monocyte-derived microvesicles (MDMVs), which can express the coagulation protein tissue factor, contribute to thrombus formation and cardiovascular disease. People living with HIV experience higher prevalence of cardiovascular disease and also exhibit increased levels of plasma microvesicles. The process of microvesicle release has striking similarity to budding of enveloped viruses. The surface protein tetherin inhibits viral budding by physically tethering budding virus particles to cells. Hence, we investigated the role of tetherin in regulating the release of MDMVs during HIV infection.

METHODS AND RESULTS: The plasma of aviremic HIV-infected individuals had increased levels of tissue factor + MDMVs, as measured by flow cytometry, and correlated to reduced tetherin expression on monocytes. Superresolution confocal and electron microscopy showed that tetherin localized at the site of budding MDMVs. Mechanistic studies revealed that the exposure of monocytes to HIV-encoded Tat triggered tetherin loss and subsequent rise in MDMV production. Overexpression of tetherin in monocytes led to morphologic changes in the pseudopodia directly underneath the MDMVs. Further, tetherin knockout mice demonstrated a higher number of circulating MDMVs and less time to bleeding cessation.

CONCLUSIONS: Our studies define a novel regulatory mechanism of MDMV release through tetherin and explore its contribution to the procoagulatory state that is frequently observed in people with HIV. Such insights could lead to improved therapies for individuals infected with HIV and also for those with cardiovascular disease.

Key Words: human immunodeficiency virus ■ immunogold ■ microvesicles ■ monocytes ■ scanning electron microscopy ■ tetherin ■ tissue factor

Age-related inflammatory diseases are dramatically increased in the HIV-infected population despite the success of combined antiretroviral treatment (cART) in repressing viral loads.^{1–3} One major contributor to this elevation is the activation of monocytes in patients with aviremic HIV, as evidenced by elevated levels of soluble monocyte activation markers sCD163⁴ and sCD14⁵ in plasma. Furthermore, both sCD163 and sCD14 have been linked to increased incidence of cardiovascular disease,^{6,7} neurocognitive disorders,^{8,9} and mortality^{10–12} in HIV-infected

individuals. One insufficiently studied mechanism of monocyte-augmented inflammation is the release of microvesicles.

Microvesicles, small membrane–derived extracellular vesicles ranging from 100 to 1000 nm in diameter, detach from the plasma membrane at lipid rafts^{13–15} and can contain surface receptors,¹⁶ proteins,¹⁷ lipids,¹⁸ mRNA,¹⁹ and mitochondria²⁰ derived from the cell of origin. Acting as signaling shuttles, microvesicles communicate with recipient cells by binding to surface receptors or by delivering cargo through endocytosis.²¹

Correspondence to: Sanjay B. Maggirwar, PhD, Department of Microbiology, Immunology and Tropical Medicine, The George Washington University, 2300 I Street NW, Washington, DC 20052. E-mail: smaggirwar@gwu.edu

Supplementary Materials for this article are available at <https://www.ahajournals.org/doi/suppl/10.1161/JAHA.120.015998>

For Sources of Funding and Disclosures, see page 13.

© 2020 The Authors. Published on behalf of the American Heart Association, Inc., by Wiley. This is an open access article under the terms of the Creative Commons Attribution-NonCommercial License, which permits use, distribution and reproduction in any medium, provided the original work is properly cited and is not used for commercial purposes.

JAHA is available at: www.ahajournals.org/journal/jaha

CLINICAL PERSPECTIVE

What Is New?

- Our data demonstrate a novel relationship between the surface protein and the release of tissue factor–positive microvesicles from monocytes during HIV infection.
- Treatment of monocytes with HIV Tat recapitulated what was observed in clinical monocytes from those with HIV: (1) increased tissue factor expression, (2) decreased tetherin expression, and (3) increased release of microvesicles.

What Are the Clinical Implications?

- Future therapies could target tetherin to modulate microvesicle release, providing a novel treatment to ameliorate inflammatory aspects relating to HIV comorbidities and potentially for other microvesicle-related inflammatory diseases as well.

Nonstandard Abbreviations and Acronyms

cART	combined antiretroviral treatment
INSTI	integrase strand transfer inhibitor
MDMVs	monocyte-derived microvesicles
MFI	median fluorescence intensity
NNRTI	nonnucleoside reverse transcriptase inhibitor
NRTI	nucleoside reverse transcriptase inhibitor
PI	protease inhibitor
TF	tissue factor

Microvesicles promote inflammation through multiple mechanisms, such as activating endothelial cells^{22,23} or augmenting coagulation through tissue factor (TF) expression.^{24,25} Higher rates of circulating microvesicles are linked to numerous inflammatory diseases,^{26–31} many of which are prevalent in the HIV-infected population.^{1–3,32} Studies have also demonstrated that microvesicles from treated HIV-infected individuals increase inflammation in endothelial cells.³³ Despite their important impact during inflammation, little is understood about the processes regulating microvesicle biogenesis and release, particularly those emerging from monocytes.

The plasma membrane protein tetherin (also referred to as BST2, CD317, and HM1.24) regulates virion release³⁴ and provides a potential unstudied mechanism of microvesicle regulation. Using its dual-membrane

domains, tetherin physically sequesters budding enveloped viruses to the cell surface. As virions bleb from the plasma membrane at lipid rafts,³⁵ either of tetherin's terminals are inserted in the envelope of the budding virion, thereby restricting viral release until both tetherin and the virion are recycled back into the cell for degradation.^{36,37} Tetherin may additionally tether microvesicles, as their egress from the cell has striking similarities to virion release, as both occur at the curvature formation of lipid rafts.^{13,35} A recently published study demonstrated that overexpression of tetherin in cultured cell lines can also tether nanoparticles (also known as exosomes) that are released when endocytic compartments fuse with the plasma membrane.³⁸ Although microparticles and nanoparticles are similar in their ability to act as signaling shuttles and induce inflammation, these particles greatly differ in their biogenesis from the secreting cell. Microparticles arise from the plasma membrane, whereas nanoparticles emerge from multivesicular bodies.³⁹ Thus, the focus of this study is to investigate tetherin's effect on microvesicle regulation.

In this report, we investigated tetherin's ability to sequester monocyte-derived microvesicles (MDMVs) to the surface of the cell during HIV infection. We demonstrated that tetherin levels are decreased on the surface of CD14+ monocytes in HIV-infected individuals receiving cART and that these levels negatively correlate with the amount of circulating MDMVs in the plasma. In vitro studies performed with primary monocytes established that treatment with the HIV-encoded protein Tat causes decreased tetherin expression on the surface of these cells and increased MDMV release. Further, a direct relationship between MDMVs and tetherin was established when mice lacking tetherin had elevated levels of circulating MDMVs and exhibited reduced time of bleeding cessation. This study investigates a novel mechanism of MDMV regulation by tetherin, discovering new targets for improved treatments in those with HIV and other microvesicle-related inflammatory diseases.

METHODS

Data that support the findings of this study are available from the corresponding author upon reasonable request.

Ethics Statement

All studies involving human samples were reviewed and approved by the University of Rochester Medical Center Research Subjects Review Board. Blood samples were acquired from adults after written informed consent in accordance with the Declaration of Helsinki. Animal studies were performed in accordance with the

Animal Welfare Act and the National Institute of Health guidelines, and protocols were reviewed and approved by the University Committee on Animal Resources of the University of Rochester Medical Center. The Association for the Assessment and Accreditation of Laboratory Animal Care International fully accredited the facilities and programs of the Vivarium and Division of Laboratory Animal Medicine of the School of Medicine and Dentistry. The data that support the findings of this study are available from the corresponding author.

Whole Blood Samples From Human Subjects

Participants with or without HIV infection were eligible for the study if they had not previously taken any nonsteroidal anti-inflammatory drugs within a week of blood donation. Blood was drawn into acid citrate dextrose buffered vacutainers (BD Biosciences, San Jose, CA). Participant demographics are reported in Table.

Flow Cytometry Analysis

Monocytes were analyzed as previously described.⁴⁰ Whole blood was fixed with paraformaldehyde (2% final concentration) followed by lysis of red blood cells using ACK RBC lysis buffer (Gibco, Los Gatos, CA). Samples were then stained with 3 μ L anti-CD16 PE Cy7 (BD Biosciences, Franklin Lakes, NJ), 8 μ L anti-CD14 PE

(BD Biosciences), and 5 μ L anti-CD317 Alexa Fluor 488 (Tetherin, Invitrogen, Grand Island, NY) for 30 minutes following acquisition using an Accuri C6 flow cytometer (BD Biosciences). In vitro flow cytometry was performed with monocytes fixed as above and stained with 5 μ L anti-CD317 Alexa Fluor 488 (Tetherin, Invitrogen) or 5 μ L anti-CD142 APC (TF, Invitrogen). Fluorescence minus one controls were used to define gates.

Microvesicles were quantified from platelet-free plasma. Whole blood was loaded onto Histopaque (Sigma Aldrich, Saint Louis, MO) and centrifuged at 1250g for 25 minutes. Platelet-poor plasma was collected and centrifuged at 5000g for 5 minutes to collect platelet-free plasma. The platelet-free plasma diluted in 0.2 μ m filtered Dulbecco's phosphate buffered saline (Sigma Aldrich, St Louis, MO) and stained with 8 μ L anti-CD14 PE, 5 μ L anti-CD14 FITC (Invitrogen) and 5 μ L anti-CD147 APC (TF, Invitrogen) for 30 minutes. Twenty-five μ L was acquired using the Accuri C6 cytometer, and sizing beads (Mega Mix, BioCytex, Marseille, France) ranging from 500 to 1000 nm were used to define the gate for microvesicles.

The mouse strain C57BL/6 was purchased from the Jackson Laboratory. The tetherin-knockout mouse strain B6.Cg-BST2^{tm1.Bsz}/J was a gift from Dr Paul Biendiaz (Rockefeller University) and was generated as previously described.⁴¹ For quantification of microvesicles in mouse plasma, blood was obtained by retro-orbital puncture. Platelet-free plasma was collected by centrifugation at 3500g for 5 minutes and stained using 0.2 μ L anti-CD115 APC (eBioscience, San Diego, CA) per sample.

Table. Donor Demographics and Characteristics

Characteristics	HIV-	HIV+
Total number of participants	20	20
Mean age, y (SD)	47 (11)	53 (9)
Sex, N (%)		
Female	12 (60)	3 (15)
Male	8 (40)	17 (85)
Race, N (%)		
Black	5 (25)	6 (30)
Hispanic	0 (0)	2 (10)
White	15 (75)	12 (60)
Mean CD4 count, cells/mm ³ (SD)		859 (239)
cART treatment, N (%)		
NRTI/PI		7 (35)
NRTI/NNRTI		6 (30)
NRTI/INSTI		6 (30)
PI/NNRTI		1 (5)
Viral load		
Undetectable, N (%)		17 (85)
Detectable, N (%), mean RNA copies/mL [SD]		3 (15%), 80 [53]

cART indicates combined antiretroviral therapy; INSTI, integrase strand transfer inhibitor; NNRTI, nonnucleoside reverse transcriptase inhibitor; NRTI, nucleoside reverse transcriptase inhibitor; and PI, protease inhibitor.

In Vitro Treatment of Monocytes and MDMV Quantification

Monocytes were isolated from HIV-negative donors by MACS CD14+ Beads (Miltenyi Biotec, Sunnyvale, CA) per manufacturer's instructions and cultured with 0.2 μ m filtered RPMI 1640 supplemented with 10% fetal bovine serum and 1% penicillin-streptomycin-glutamine. When specified, cells were treated with 500 nmol/L HIV viral full-length recombinant 101 amino acid Tat (kindly provided by the University of Rochester Center for AIDS Research), a dose used previously in the literature in vitro.⁴²⁻⁴⁴ The National Institutes of Health AIDS Reagent Program provided HIV treatment drugs raltegravir (5 μ mol/L), tenofovir disoproxil fumarate (5 μ mol/L), and emtricitabine (5 μ mol/L). Dimethyl sulfoxide (Sigma Aldrich) was used as vehicle control. After 18 hours, monocytes were processed for flow cytometry as described above. For Tat treatments, cells were stained for surface tetherin or TF as described above. For HIV drug treatments, cells were stained with 10 μ L anti-CD142-FITC (TF, Miltenyi Biotec, Bergisch Gladbach, Germany).

Before quantification, cells and debris were depleted from the media by centrifugation. Where specified, vesicles were quantified using a Nanosight NS300 (Malvern Instruments, Amesbury, UK) and subsequently analyzed by NanoSight Tracking Analysis (Malvern Instruments). Briefly, media were diluted 1:10 in 0.2 μm filtered Dulbecco's phosphate buffered saline, and 5 videos lasting 30 seconds in duration were acquired. The number of background vesicles detected in the filtered media were subtracted for each experiment. Alternatively, media were stained with FilmTracer calcein green biofilm stain (Molecular Probes, Eugene, OR) according to manufacturer's specifications or 5 μL Annexin V APC (BD Biosciences) and 8 μL CD14 PE. Before Annexin V staining, microvesicles and RPMI was spun at 20 000g for 30 minutes and resuspended in 100 μL Annexin V binding buffer (BD Biosciences). Fifteen microliters of media was acquired on the BD Accuri C6 as described above.

mRNA Quantification

RNA from either Tat treated or nontreated cells was harvested using Trizol (Invitrogen) per the manufacturer's instructions, and contaminating DNA was digested using DNase I (Invitrogen). The iScript cDNA Synthesis Kit (Bio-Rad, Hercules, CA) was used to synthesize RNA into cDNA as per the manufacturer's instructions. Power SYBR Green PCR Master Mix (Applied Biosystems, Foster City, CA) along with previously published primers for tetherin⁴⁵ or the housekeeping gene GAPDH⁴⁶ were analyzed on CFX Connect Real Time System (Bio-Rad).

Lentivirus Transduction of Primary Monocytes

Expression plasmids pCDH-CMV-MCS-EF1 PURO (System Biosciences, Palo Alto, CA) containing full-length wild-type tetherin transcripts were kindly provided by Dr Jean Gustin.^{47,48} The tetherin expression plasmids, along with the packing plasmid pCMV4- Δ 89.2 and the envelope plasmid VSV-G (vesicular stomatitis virus glycoprotein), were used to produce recombinant lentivirus vectors in HEK 293T cells. These cells were cultured in Dulbecco's Modified Eagle Medium supplemented with 10% fetal bovine serum and 1% penicillin-streptomycin-glutamine. Viruses were then concentrated using PEG6000 (Sigma Aldrich),⁴⁹ and titered by using optical density as outlined.⁵⁰ Finally, the primary cultures of human monocytes were transduced as recently described.⁵¹

Electron Microscopy Imaging

For scanning electron microscopy, monocytes were isolated as described above and plated onto glass

poly-L-lysine-coated coverslips. Monocytes were treated with 20 ng/mL tumor necrosis factor alpha (Sigma) for 18 hours to induce microvesicle formation. Cells for immunogold labeling were then fixed with 1% paraformaldehyde for 30 minutes followed by blocking in 1% bovine serum albumin and 1% goat serum in Dulbecco's phosphate buffered saline for 30 minutes. Cells were incubated in a 1:500 dilution of goat anti-tetherin antibody (National Institutes of Health AIDS Reagents Program) at room temperature for 1 hour followed by 2 hours of goat anti-rabbit IgG H&L 40 nm gold (Abcam, Cambridge, England). Additional monocytes were also infected by lentiviral transduction at 1000 multiplicity of infection with 5 $\mu\text{g}/\text{mL}$ polybrene (Santa Cruz Biotechnology, Santa Cruz, CA) for 24 hours and treated with HIV Tat (100 nmol/L) for 1 hour, followed by fixation in 2.5% glutaraldehyde in 0.1 mol/L sodium cacodylate buffer overnight. Both immunogold-labeled and Tat treated monocytes were postfixed in buffered 1.0% osmium tetroxide. All coverglasses were then through a graded series of ethanol to 100% (3x) followed by graded series of 100% ethanol and hexamethyldisilazane and final series of 100% hexamethyldisilazane (3x). This last solution of 100% hexamethyldisilazane was evaporated overnight. Finally, immunogold-labeled coverglasses were mounted onto aluminum stubs and sputter coated for 15 seconds with platinum and all other coverglasses were sputter coated with gold for 90 seconds and imaged using a Zeiss Supra 40VP Field Emission scanning electron microscope (Oberkochen, Germany).

Superresolution Confocal Microscopy Imaging

Primary monocytes were isolated as specified above, fixed using 2% paraformaldehyde, and stained for tetherin as specified for scanning electron microscopy, followed by secondary goat anti-rabbit H&L Alexa Fluor 488 (Molecular Probes). The cellular membrane was labeled using Cell Mask Red (Invitrogen). Images were acquired using a Leica (Wetzlar, Germany) TCS SP8 confocal microscope with Leica HC PL APO CS2 \times 63 magnification with 1.40 numerical aperture at room temperature. The acquisition software used was Leica LAS X (BETA) 3.5.0.18154 with Leica detectors HyD 505 to 588 nm in standard mode and HyD 654 to 731 nm in standard mode. Images were processed with Leica LIGHTNING Image Information Extraction.

Tail Bleed Assay

The time to bleeding cessation from mouse tail was performed as previously outlined.^{52,53} Briefly, mice over 8 weeks of age were anesthetized completely

before 2 mm was cut from the tip of the tail. Time was recorded from the time of the cut to when bleeding ceased.

Statistical Analysis

All statistical analyses were performed using Prism (GraphPad Software, La Jolla, CA). Specific tests used to compare data are stated in figure legends. Statistical significance indicated as * $P < 0.05$, ** $P < 0.01$, and *** $P < 0.001$ shown in figures; all error bars shown in figures represent the SEM. In results, means are provided with \pm SEM.

RESULTS

Decreased Tetherin Expression on CD14+ Monocytes Correlates to Increased Levels of Circulating MDMVs During HIV Infection

Because tetherin has been demonstrated to sequester virus particles, which are of similar size and biogenesis as MVs, we investigated whether tetherin also regulates MV release. Thus, tetherin expression on the surface of monocytes was measured in 20 HIV-positive and 20 HIV-negative individuals (Table 1). Whole blood from donors was fixed and stained with the monocyte markers CD14 and CD16 to separate monocytes into their subsets, classical (CD14^{high},CD16^{low}), intermediate (CD14^{high},CD16^{low}), and nonclassical (CD14^{low},CD16^{high}). Tetherin expression on the surface of cells was measured by flow cytometry. By both median fluorescence intensity (MFI) and percentage, tetherin expression was significantly decreased the CD14+ classical (MFI HIV–, 6091 \pm 328.3 versus MFI HIV+ mean, 4677 \pm 283.4; $P = 0.0009$) (percent HIV–, 84.72 \pm 4.226 versus percent HIV+, 70.58 \pm 4.483; $P = 0.0471$) and intermediate CD14+ subsets (MFI HIV–, 5947 \pm 256.2 versus MFI HIV+, 4829 \pm 262.1; $P = 0.0114$) (percent HIV–, 82.9 \pm 3.135 versus percent HIV+, 55.21 \pm 5.479; $P < 0.0001$), but not in the CD14– nonclassical subset (MFI HIV–, 2800 \pm 280.4 versus MFI HIV+, 2326 \pm 170.5; $P = 0.5130$) (percent HIV–, 27.74 \pm 4.166 versus percent HIV+, 13.94 \pm 2.247; $P = 0.0547$) (Figure 1A and 1B). Such a decrease was continually observed in combined population of CD14+ monocytes derived from HIV-infected individuals (MFI HIV–, 5961 \pm 332.5 versus MFI HIV+, 4664 \pm 260.3; $P = 0.0039$) (percent HIV–, 89.02 \pm 3.597 versus percent HIV+, 72.45 \pm 4.187; $P = 0.0007$) (Figure 1C and 1D). Patient characteristics, including, sex (male, 5209 \pm 283 versus female, 5484 \pm 412.9; $P = 0.5742$), age (MFI, 3.709 \pm 0.01946 versus age, 1.685 \pm 0.01615; $P = 0.349$), race/ethnicity (White, 4962 \pm 261.7 versus Hispanic, 5848 \pm 930.5;

$P = 0.6718$; or versus Black, 5209 \pm 468.1; $P = 0.8771$; Hispanic versus Black; $P = 0.8277$), viral load (undetectable, 4693 \pm 298.1 versus detectable, 4496 \pm 494.4; $P = 0.7947$), CD4+ T-cell count (MFI, 3.657 \pm 0.0233 versus CD4, 2.919 \pm 0.02716; $P = 0.071$, and specific cART regimen (nucleoside reverse transcriptase inhibitor [NRTI]/protease inhibitor [PI], 4850 \pm 502.2 versus NRTI/nonnucleoside reverse transcriptase inhibitor [NNRTI], 4187 \pm 277.5; $P = 0.5407$; or versus NRTI/integrase strand transfer inhibitors [INSTI], 4571 \pm 472.7; $P = 0.8935$; NRTI/NNRTI versus NRTI/ISNTI; $P = 0.8212$) did not influence tetherin levels (Figure S1A).

Circulating microvesicles were quantified from the same individuals as above. Staining for CD14 and TF allowed enumeration of inflammatory MDMVs using flow cytometry. To ensure the authenticity of CD14+ only microvesicles, the blood samples were stained with 2 separate CD14-specific antibodies that were raised against distinct epitopes and were distinguished by different fluorophores. Our analyses showed that the estimation of microvesicles in a given sample was comparable regardless of antibodies used (fluorescein isothiocyanate, 1 \pm 0.2739 versus phycoerythrin, 1.022 \pm 0.1954; $P < 0.0001$) (Figure S2A). Furthermore, the number of CD14+ microvesicles from each donor correlated when 2 different instruments were used to enumerate (Nanosight, 1.003 \pm 0.03917 versus Accuri, 0.9785 \pm 0.1975; $P = 0.0500$) (Figure S2B).

When microvesicles carrying multiple markers were quantified, HIV-infected individuals were found to contain increased levels of circulating TF+ (HIV–, 4.871 \pm 0.07979 versus HIV+, 5.121 \pm 0.08974; $P = 0.0441$) or CD14+ microvesicles (HIV–, 5.101 \pm 0.07681 versus HIV+, 5.412 \pm SEM 0.08396; $P = 0.0095$) (Figure 1E and 1F), in agreement with previous studies.^{33,54} Furthermore, CD14+ TF+ microvesicles were also increased in HIV-infected individuals (HIV–, 4.466 \pm 0.06587 versus HIV+, 4.79 \pm 0.09423; $P = 0.0068$) (Figure 1G). In this cohort, sex (TF+ male, 5.451 \pm 0.08348 versus TF+ female, 5.338 \pm 0.1033; $P = 0.4022$) (CD14+ male, 5.278 \pm 0.07124 versus female, 5.203 \pm 0.1133; $P = 0.3249$) (CD14+ TF+ male, 4.637 \pm 0.07684 versus CD14+ TF+ female, 4.593 \pm 0.106; $P = 0.4919$), age (age, 1.684 \pm 0.01697 versus TF+ 5.406 \pm 0.06469; $P = 0.589$; or versus CD14, 5.248 \pm 0.06149; $P = 0.206$; or versus CD14+ TF+, 4.62 \pm 0.06177; $P = 0.220$), race/ethnicity (TF+ White, 5.408 \pm 0.07736 versus TF+ Hispanic, 5.279 \pm 0.1133; $P = 0.9032$; or versus TF+ Black, 5.43 \pm 0.15; $P = 0.9892$; TF+ Hispanic versus TF+ Black; $P = 0.8846$) (CD14+ White, 5.258 \pm 0.08142 versus CD14+ Hispanic, 5.041 \pm 0.07638; $P = 0.7264$; or versus CD14+ Black, 5.263 \pm 0.106; $P = 0.9995$; CD14+ Hispanic versus CD14+ Black; $P = 0.7378$) (CD14+ TF+

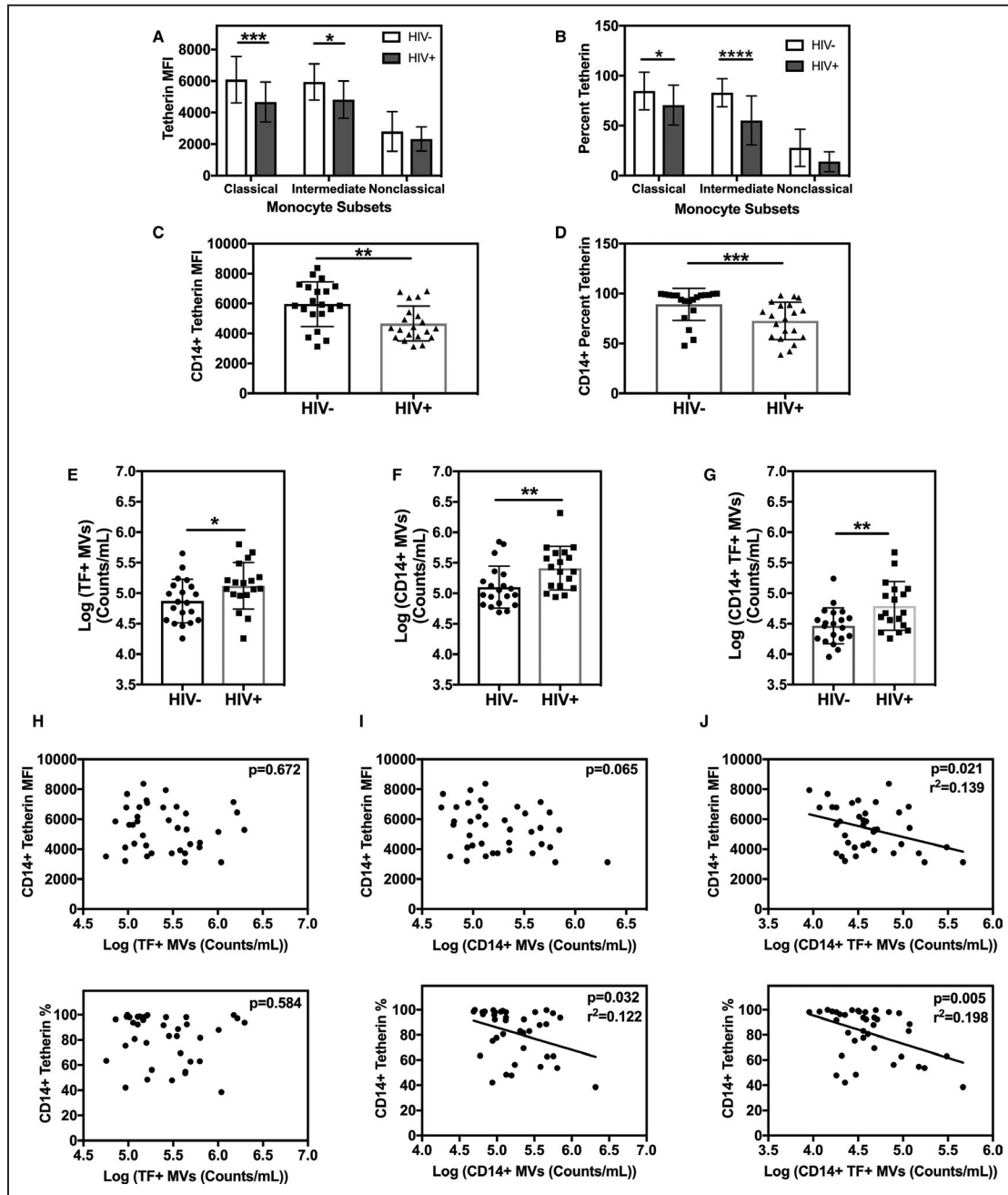


Figure 1. Decreased surface tetherin levels on CD14+ monocytes correlate with increased circulating CD14+ microvesicles during HIV infection.

A through D, Flow cytometric analysis of surface tetherin expression on monocytes in HIV- (N=20) and HIV+ (N=20) donors. Monocytes were separated into their subtypes by the markers CD14 and CD16, and levels of tissue factor (TF) were quantified. Tetherin levels are reported by median fluorescence intensity (MFI; **A** and **C**) or percent (**B** and **D**). Two-way ANOVA test with Sidak's multiple comparison test was used to compare subsets between HIV- and HIV+ (**A** and **B**). The CD14+ classical and intermediate subsets are shown pooled together (**C** and **D**). An unpaired t test was used to compare MFI (**C**) and the Mann-Whitney test was used to compare percentage (**D**) of tetherin between HIV- and HIV+. **E through G,** Circulating microvesicles in donor plasma was quantified by volumetric flow cytometry quantification in HIV- (N=20) and HIV+ (N=18) donors. Microvesicles expressing tissue factor (TF, **E**), CD14 (**F**), or both TF and CD14 (**G**) were enumerated. Unpaired t tests were performed to compare microvesicles between HIV- and HIV+. **H through J,** Pearson analysis was performed to evaluate the correlation between the amount of CD14+ MVs to tetherin levels, in terms of both MFI and percent (N=38), *p<0.05, **p<0.01, ***p<0.001 and ****p<0.0001.

White, 4.63 ± 0.07693 versus CD14⁺ TF⁺ Hispanic, 4.306 ± 0.04846 ; $P=0.4880$; or versus CD14⁺ TF⁺ Black, 4.657 ± 0.1175 ; $P=0.9816$; CD14⁺ TF⁺ Hispanic versus CD14⁺ TF⁺ Black; $P=0.4773$) CD4 cell (CD4 2.926 ± 0.02949 versus TF⁺ 5.543 ± 0.08299 ; $P=0.077$; or versus CD14⁺ 5.412 ± 0.08396 ; $P=0.375$; or versus CD14⁺ TF⁺, 4.79 ± 0.09423 ; $P=0.929$) or viral counts (TF⁺ undetectable, 5.551 ± 0.0977 versus TF⁺ detectable, 5.503 ± 0.127 ; $P=0.8346$) (CD14⁺ undetectable, 5.39 ± 0.09738 versus CD14⁺ detectable, 5.523 ± 0.142 ; $P=0.4265$) (CD14⁺ TF⁺ undetectable, 4.752 ± 0.1106 versus CD14⁺ TF⁺ detectable, 4.984 ± 0.05132 ; $P=0.3754$) did not significantly influence CD14⁺ microvesicle (Figure S1B), TF⁺ microvesicles (Figure S1C), or CD14⁺ TF⁺ microvesicle levels (Figure S1D). CD14⁺ TF⁺ did not differ in regards to cART regime (NRTI/PI, 4.887 ± 0.09555 versus NRTI/NNRTI, 4.555 ± 0.1166 ; $P=0.3229$; or versus NRTI/integrase strand transfer inhibitor [INSTI], 4.979 ± 0.2113 ; $P=0.9016$; NRTI/NNRTI versus NRTI/INSTI; $P=0.1724$); however, CD14⁺ (NRTI/PI, 5.428 ± 0.1114 versus NRTI/NNRTI, 5.156 ± 0.1334 ; $P=0.3520$; or versus NRTI/INSTI, 5.658 ± 0.1472 ; $P=0.4345$; NRTI/NNRTI versus NRTI/INSTI; $P=0.0477$) and TF⁺ MVs (NRTI/PI, 5.644 ± 0.1643 versus NRTI/NNRTI, 5.222 ± 0.1249 ; $P=0.0890$; or versus NRTI/INSTI, 5.736 ± 0.07388 ; $P=0.8593$; NRTI/NNRTI versus NRTI/INSTI; $P=0.0354$) did significantly differ when different types of cART were compared (Figure S1B and S1C). However, this is unlikely because of direct effects from integrase inhibitors themselves, as primary monocytes treated with the integrase inhibitor raltegravir [RAL] did not increase expression of tissue factor (not treated [NT], 6.016 ± 1.57 versus dimethyl sulfoxide, 7.28 ± 0.1168 ; $P=0.8058$; or versus RAL, 4.202 ± 1.06 ; $P=0.3527$; or versus RAL+ Tenofovir disoproxil fumerate [TDF] + Emtricitabine [FTC], 4.87 ± 1.141 ; $P=0.2165$) or release of microvesicles (NT versus dimethyl sulfoxide, 0.8878 ± 0.1355 ; $P=0.9517$; or versus RAL, 0.9489 ± 0.1673 ; $P=0.9947$; or versus RAL+ TDF+FTC, 0.9291 ± 0.3123 ; $P=0.9865$) (Figure S3).

Next, in an effort to investigate if there was a link between microvesicle quantities and tetherin levels on CD14⁺ monocytes, statistical correlation analyses were performed. TF⁺ microvesicles did not correlate with levels of tetherin on CD14⁺ monocytes (TF⁺ microvesicles, 5.406 ± 0.06469 versus MFI, 5367 ± 241.3 ; $P=0.672$; or versus percent, 81.52 ± 3.12 ; $P=0.584$) (Figure 1H), likely because other cells besides monocytes can contribute to this population of microvesicles.^{24,55} However, CD14⁺ tetherin levels were found to be negatively correlated with both CD14⁺ (5.248 ± 0.06149 versus MFI, 5367 ± 241.3 ; $P=0.065$; or versus percent, 81.52 ± 3.12 ; $P=0.032$) and CD14⁺ TF⁺ microvesicle levels (4.62 ± 0.06177 MFI, 5367 ± 241.3 ;

$P=0.021$; or versus percent, 81.52 ± 3.12 ; $P=0.005$) (Figure 1I and Figure 1J). These data demonstrate that there is a direct relationship between tetherin expression on the surface of monocytes and MDMV release in HIV-infected subjects.

Tetherin is Colocalized With Microvesicles on the Surface of Monocytes

Because of the correlation between tetherin levels and MDMV production in monocytes, we next determined whether tetherin was physically localized next to microvesicles on monocytes. Primary monocytes were isolated from healthy HIV-negative donors and treated with 20 ng/mL tumor necrosis factor alpha to induce microvesicle formation. Cells were fixed, immunogold labeled for tetherin, and processed for electron microscopy. Consistent with scanning electron microscopy imaging of extracellular vesicles reported in other cells,^{56,57} vesicles of similar size and characteristics as microvesicles were observed on the surface of monocytes. Tetherin was found to be localized close to these microvesicles (Figure 2A, arrows). These results were further verified by performing superresolution confocal microscopy (Figure 2B; Figure S4). The images acquired by these methods also show that tetherin is localized directly at the base of microvesicle-sized vesicles on the surface of monocytes, overall demonstrating that tetherin is in the correct position to keep microvesicles arrested on the cell surface.

Exposure to HIV-Encoded Tat Decreases Tetherin Surface Expression on Primary Monocytes With Concomitant Increase in Microvesicle Production

Tetherin is well known to be downregulated by the HIV viral protein Vpu.³⁴ However, Vpu is a late-expressed protein and is not secreted outside the cell.⁵⁸ Hence, it is extremely unlikely that monocytes, which rarely harbors HIV in subjects on suppressive cART,^{59,60} will be exposed to Vpu in aviremic individuals. This led us to investigate if other viral proteins could affect tetherin expression. The HIV viral protein Tat is an early expressed protein that is secreted by infected cells in detectable amounts in the serum of cART-treated individuals.^{61,62} Furthermore, cells (including monocytes) exposed to Tat have been shown to exhibit a wide variety of changes at the transcriptional level.⁶³ To investigate whether Tat could be modulating tetherin expression, we isolated primary monocytes from HIV-negative donors and exposed them to Tat. Short 4-hour exposures to Tat did not affect tetherin expression (NT, 50.63 ± 16.58 versus Tat, 57.43 ± 17.93 ; $P=0.2328$) (Figure S5A); however, Tat treatment of monocytes for

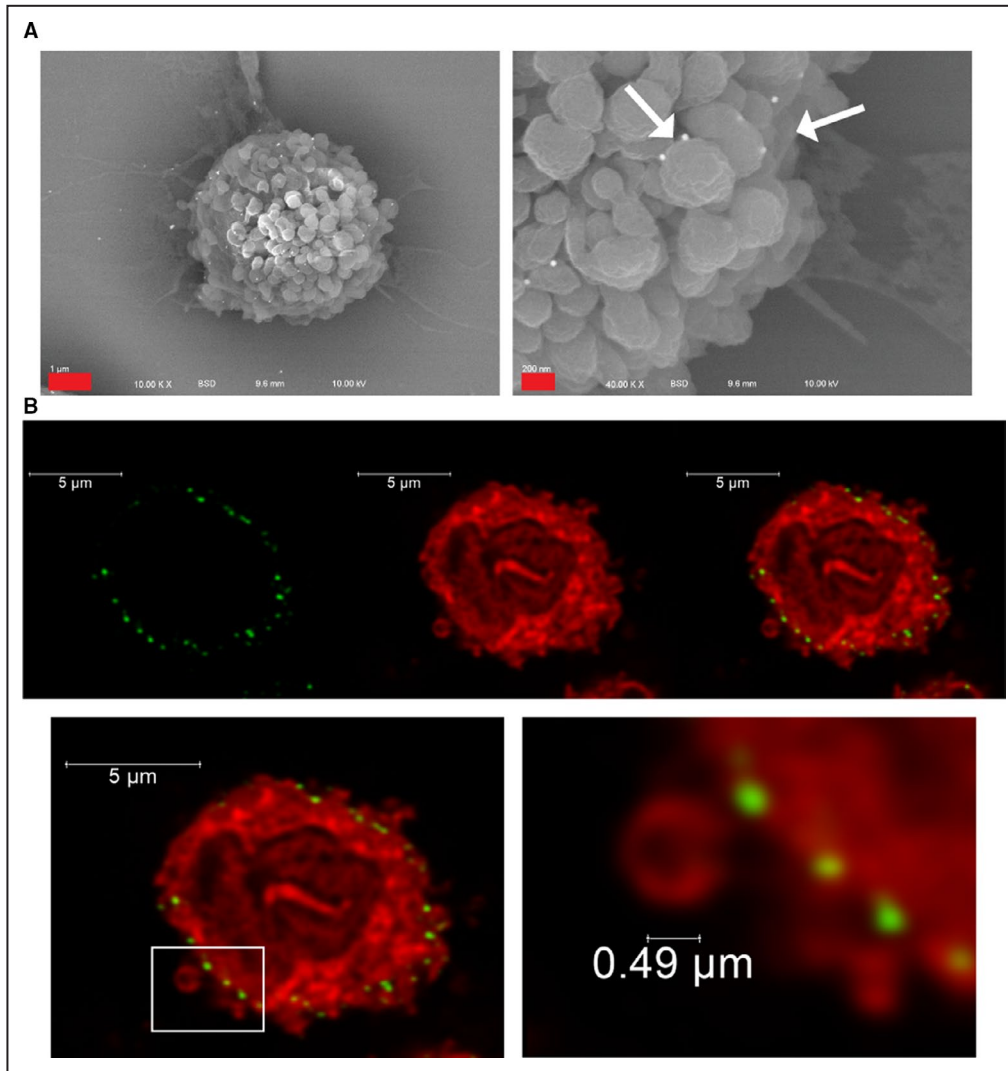


Figure 2. Tetherin localizes at the site of budding microvesicles on the surface of monocytes.

A, Primary monocytes were isolated from HIV⁻ donors followed by treated with 20 ng/mL tumor necrosis factor alpha overnight to induce microvesicle secretion. Cell were then fixed and stained using immunogold labeling for tetherin, located next to budding microvesicles (arrows). Red bar in left image denotes 1 $\mu\text{mol/L}$, and red bar in right image denotes 200 nm. **B**, Primary monocytes were isolated as above, fixed, and stained for tetherin and the cell membrane was labeled with Cell Mask Red. Tetherin again appeared next to budding microvesicles on the cell membrane (arrows). White bars on top images denote 5 μm and white bar on bottom images denote distances as stated.

18 hours significantly decreased cell surface tetherin expression (MFI NT, 9624 ± 424 versus Tat, 4862 ± 634 ; $P=0.0006$) (percent NT mean, 88.1 ± 3.133 versus Tat, 46.67 ± 9.204 ; $P=0.0011$) (Figure 3A) (NT, 54.38 ± 7.851 versus 500 nmol/L 29.01 ± 4.259 ; $P=0.0240$, or versus 100 nmol/L 35.93 ± 3.914 ; $P=0.1119$; or versus 50 nmol/L 37.83 ± 5.581 ; $P=0.1670$; or versus 5 nmol/L 49 ± 9.256 ; $P=0.8968$) (Figure S5B) as well as at the mRNA level (0.19 ± 0.07506 ; $P=0.0004$) (Figure 3B). In addition to microvesicle quantification, we also sought to quantify expression of TF on monocytes in response to Tat because of TF+ microvesicles' ability to augment coagulation.^{24,64,65} Furthermore, monocytes during HIV infection,

even while patients are undergoing cART, express high levels of TF,⁶⁶ and thus, we investigated whether Tat could be contributing to this observed increase in expression. Surface TF expression increased on monocytes exposed to Tat (MFI NT, 694.1 ± 12.12 versus Tat, 963.4 ± 26.99 ; $P=0.0006$) (percent NT, 28.89 ± 2.95 versus Tat, 47.21 ± 2.355 ; $P=0.0003$) (Figure 3C).

To investigate whether Tat also increased MDMV release, media were collected from Tat treated monocytes, and the number of released vesicles was enumerated. Microvesicles were quantified by NanoSight Tracking Analysis, measuring 200 to 1000 nm in diameter to exclude exosomes.⁶⁷ Upon Tat treatment,

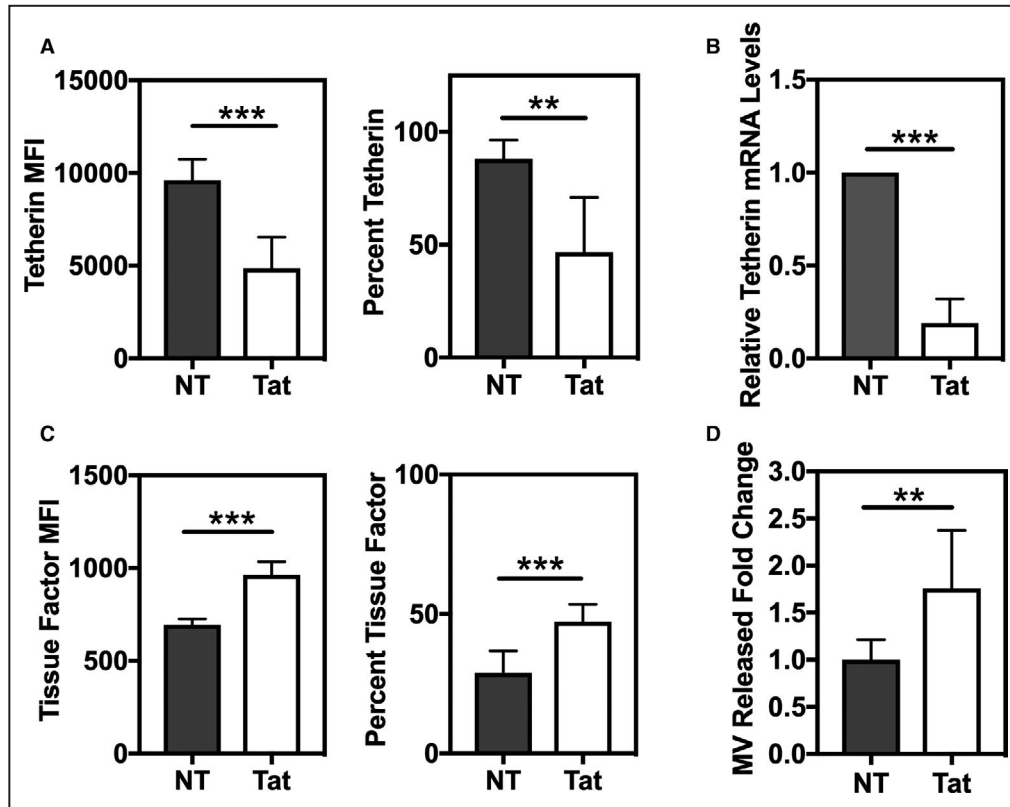


Figure 3. HIV Tat decreases levels of tetherin on the surface of monocytes and increases tissue factor and microvesicle release.

Primary monocytes from HIV⁻ donors were exposed to the HIV viral protein Tat (500 nmol/L) for 18 hours. **A** and **C**, Cells were then fixed and levels of tetherin (**A**) or tissue factor (**C**) on the surface of the cells were measured by flow cytometry and compared to cells that were not treated (NT). Expression levels were compared using either MFI followed by analysis with a Mann–Whitney test or percent expression followed by unpaired t test comparison. **B**, mRNA was isolated from NT or Tat-treated monocytes and the levels of tetherin mRNA transcripts were compared to the housekeeping gene GAPDH. Unpaired t test was used to compare NT to Tat expression levels of mRNA. **D**, The number of microvesicles released from monocytes was quantified by the NS300 and Nanosight Tracking Analysis with 5 videos each lasting 30 seconds. Unpaired t test was used to compare NT to Tat. Data for all experiments in this figure were performed with 3 biological replicates with 2 to 3 technical replicates per group. In (**B**) technical replicates were averaged per biological sample. In (**A**, **C**, and **D**) all data points for each technical replicate from 3 biological replicates were included (N=7–9), ***p*<0.01, ****p*<0.001.

monocytes significantly increased release of MDMVs into the media (nontreated, 1 ± 0.07099 versus Tat, 1.758 ± 0.205 ; *P*=0.003) (Figure 3D). MDMVs from nontreated and Tat-treated monocytes were of similar size in both mean (nontreated, 279.8 ± 9.157 versus Tat, 283.4 ± 5.34 ; *P*=0.6477) and mode (nontreated, 238 ± 0.8602 versus Tat, 237.3 ± 2.106 ; *P*=0.7431) diameter (Figure S6). Additionally, to investigate whether microvesicles were being quantified on the NS300 or if it was analyzing erroneous matter in the media, media from monocytes incubated overnight was compared with the RPMI in which the monocytes were suspended. Media from cells contained significantly more microvesicles as measured by calcein green, demonstrating these microvesicles were membrane enclosed (RPMI, $14\,400 \pm 3150$ versus Cell Media, $71\,511 \pm 5389$; *P*=0.0008) (Figure S7A). Additionally, there were

more microvesicles in the media from cells that had the microvesicle marker Annexin V alone (RPMI, $18\,371 \pm 2605$ versus Cell Media, $137\,784 \pm 31\,781$, *P*=0.0200) (Figure S7B) or in combination with the monocyte marker CD14 (RPMI, 1788 ± 384 versus Cell Media, 6892 ± 903.6 ; *P*=0.0065) (Figure S7C). Taken together, monocytes treated with HIV Tat in vitro corroborated with monocytes isolated from HIV-positive subjects in respect to their (1) decreased surface tetherin expression, (2) increased release of MDMVs, and (3) increased surface TF expression.

The relationship between tetherin and MDMVs was further examined by performing electron microscopy. Monocytes were first infected with a lentivirus vectors either containing a cassette expressing wild-type tetherin or nothing (empty vector). After infection, cells were treated with HIV Tat to observe morphological changes.

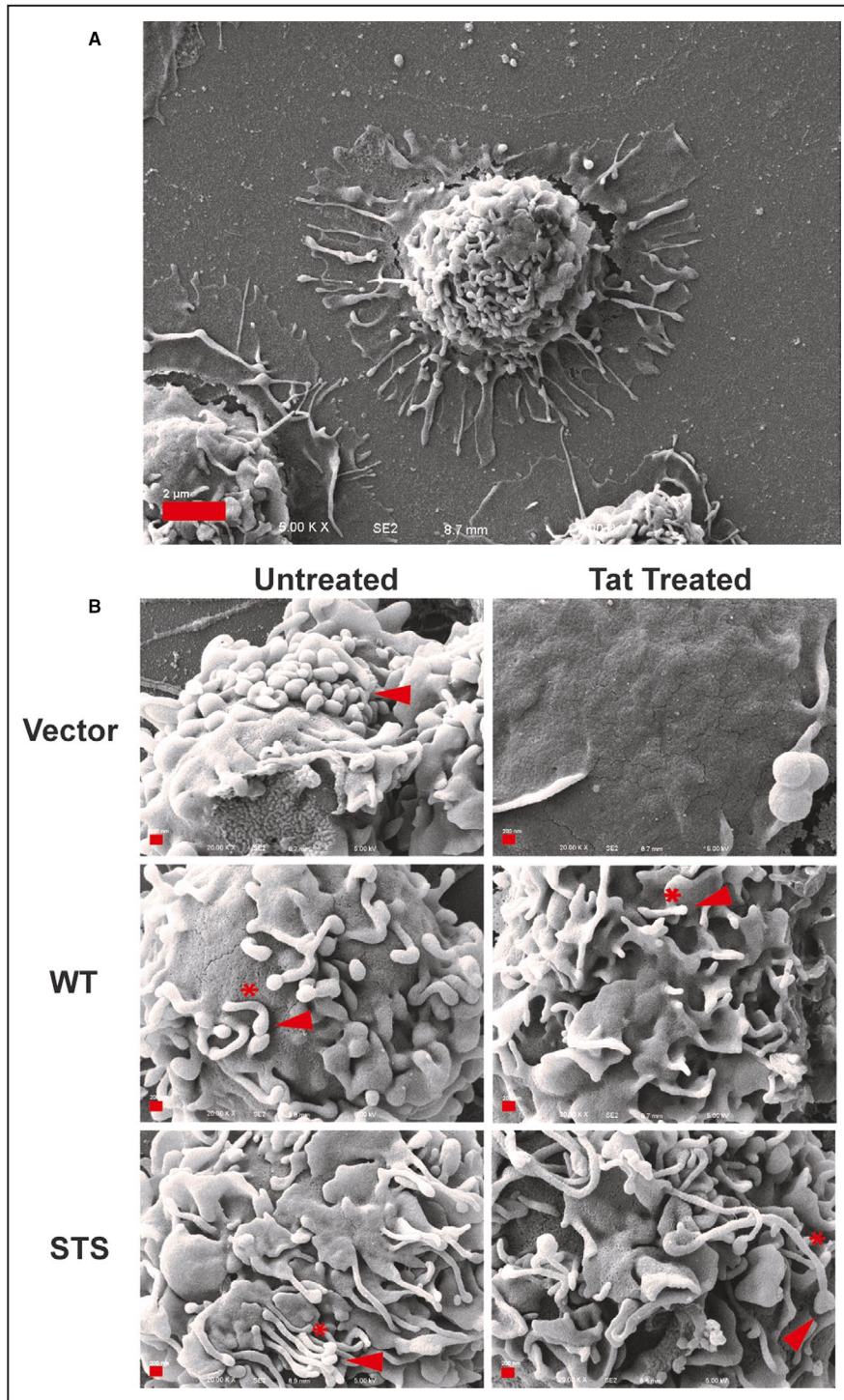


Figure 4. Scanning electron microscopy morphology of monocytes overexpressing tetherin.

Primary monocytes were isolated and infected with lentiviral vector to over express tetherin. Either an empty vector (Vector) or wild-type (WT) tetherin. Cells were either left untreated or exposed to a low level of HIV Tat (100 nmol/L) for 1-hour prior fixation and preparation for scanning electron microscopy imaging. (A) Monocytes displayed typical morphology, with large ruffles and protrusions. Red bar denotes 2 μ m. (B) Microvesicle-sized and shaped vesicles (red arrows) disappeared from the surface of Tat-treated cells. Tubular structures below vesicles (red asterisk) are visualized upon tetherin overexpression. Red bars denote 200 nm.

Under normal conditions, monocytes display large ruffles (lamellipodia) and microvesicles on their surface (Figure 4A and 4B, vector untreated, arrowheads; Figure S8). Monocytes overexpressing tetherin wild-type (WT) exhibited a morphology wherein the cells displayed abundant tubular structures (pseudopodia, Figure 4B, WT untreated, asterisks). Further, protrusions that match microvesicles in both size and morphology were located on the ends of pseudopodia (Figure 4B, WT, arrowheads, asterisk), suggesting these structures are where biogenesis and release of microvesicles occurs. These data align with other reports where microvesicles have been found on the ends of pseudopodia in scanning electron microscopy images of platelet-derived microvesicles.^{68,69} These microvesicle structures disappeared upon treatment with Tat (Figure 4B, vector and WT Tat-treated). These images visualize the close relationship of tetherin overexpression with extended pseudopodia capped with microvesicles. These data support the direct connection in Tat-mediated microvesicle release through tetherin downregulation demonstrated in Figure 3.

Tetherin Deficient Mice Exhibit Higher Numbers of Circulating MDMVs and Reduced Tail Bleeding Time

To further investigate the direct role of tetherin in microvesicles sequestration, we collected blood from a

retro-orbital puncture of tetherin-deficient knockout mice, as well as age- and sex-matched C57/BL6 mice that expressed wild-type tetherin. Tetherin knockout mice had significantly higher levels of circulating MDMVs in blood compared with their WT counterparts (WT, $520\,873 \pm 182\,698$ versus KO, $1\,007\,040 \pm 101\,256$; $P=0.0356$; Figure 5A). These data demonstrate the direct role of tetherin in MDMV sequestration.

MDMVs have been shown to play a significant role in coagulation, and thus we measured the time required for the bleeding cessation in mice via tail bleed assays. Bleeding cessation occurred rapidly in tetherin knockout mice, as compared with tetherin wild-type mice, with concomitant changes in the number of circulating MDMVs (WT, 200.5 ± 39.06 versus KO, 97.33 ± 13.4 ; $P=0.0316$) (Figure 5B). It is unlikely that platelet activation is influencing the faster bleeding cessation for tetherin knockout mice since their platelets contain the same levels of activation compared with their wild-type counterparts (WT, 4.467 ± 0.3844 versus KO, 3.35 ± 0.75 ; $P=0.2321$; Figure S9). The data presented here strongly suggest that tetherin directly affects MDMV release, which can lead to an increased procoagulatory state.

DISCUSSION

Despite the success of cART in controlling viral loads, individuals infected with HIV still suffer from numerous inflammatory diseases that are greatly augmented by

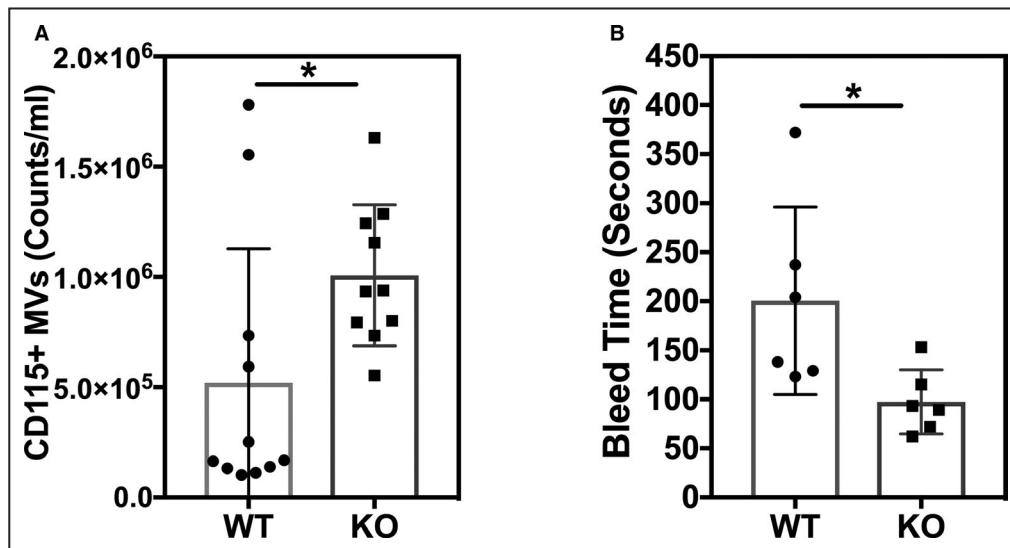


Figure 5. Mice lacking tetherin increase monocyte-derived microvesicles (MDMV) release and take less time for bleeding cessation.

A, Blood was taken from age and sex matched wild-type (WT) or tetherin knockout mice via retro-orbital bleed (N=10–11 per group). Plasma was isolated by centrifugation, stained for CD115+, and MDMVs were enumerated by flow cytometry. Unpaired t test was performed to compare number of MDMVs between WT and knockout mice. **B**, Tail bleed measurements were taken from WT or tetherin knockout mice (N=6 per group) and compared using unpaired t test. The time for bleeding cessation was measured from the beginning of the incision to when bleeding ceased, * $p < 0.05$.

monocyte activation.^{1–4,10} Monocytes exacerbate inflammation by releasing microvesicles; however, the mechanism by which microvesicles are released has remained largely unknown. In this current study, we identified a novel mechanism of microvesicle regulation through the surface protein tetherin, which plays an integral role in restricting microvesicle budding from monocytes during HIV infection. Our results demonstrated a direct correlation between decreased tetherin levels and increased circulating MDMVs in both HIV clinical samples and a tetherin knockout mouse model. Furthermore, we demonstrated that the HIV viral protein Tat decreases tetherin levels and increases microvesicle release from monocytes, suggesting that Tat contributes to the decreased tetherin levels observed in HIV individuals.

Our study further established that HIV Tat increases *in vitro* TF expression on monocytes, while our clinical data showed an increase of TF+ MDMVs in the circulation of HIV-infected individuals. The increase in TF+ microvesicle levels is particularly important during inflammation because of TF's promotion of the extrinsic coagulation cascade leading to clot-forming fibrin and platelet activation.⁷⁰ Indeed, previous studies have stressed the importance of TF+ microvesicles by demonstrating that TF expression bolsters microvesicles' ability to induce coagulation and increase thrombus size.^{24,64,65} Concurrent with these findings, we demonstrated that tetherin knockout mice had increased circulating levels of MDMVs that functionally resulted in rapid bleeding cessation. These procoagulatory TF+ MDMVs have important implications during HIV infection, as HIV-positive individuals have higher incidences of coronary heart disease⁷¹ and myocardial infarctions.⁷² Understanding the impact and regulation of TF+ MDMVs could prove pivotal for developing new treatments.

The discovery that Tat can regulate tetherin is pertinent since circulating Tat remains present in the blood of HIV-infected individuals receiving cART treatment^{61,62} and thus can mediate inflammation. Previous studies have also thoroughly established Tat as a proinflammatory protein that regulates cellular protein expression through a variety of mechanisms. For example, Tat translocates through the nuclear membrane⁷³ and binds to nuclear factor kappa light-chain enhancer of activated B cells promoter elements to downregulate the expression of host proteins.⁷⁴ The tetherin promoter contains nuclear factor kappa light-chain enhancer of activated B cells-responsive elements,⁷⁵ and thus could be occupied by Tat, thereby decreasing tetherin transcription. Alternatively, Tat has been shown to activate the MyD88 immune signaling pathway,⁷⁶ which negatively regulates tetherin.⁷⁷ Ultimately, identifying the mechanism by which Tat regulates tetherin will provide insight into how HIV evades host antiviral

response and may indicate another potential target for future therapies.

Our studies indicate a novel mechanism of inhibiting MDMV release by tetherin, a protein that act as a physical tether and is already highly documented to restrict virus particle release.^{78–81} Microvesicles and virus particles have similar biogenesis, both emerging from the plasma membrane at lipid rafts where tetherin's glycosylphosphatidylinositol anchor is localized,⁸² suggesting that tetherin could act as a physical tether for MDMVs as well. Our data indeed demonstrate that tetherin was appropriately localized at the cell membrane to physically sequester MDMVs. Further, cells overexpressing tetherin had increased pseudopodia with microparticle-sized vesicles on the ends. Monocytes could feasibly express smaller versions of these tetherin-induced pseudopodia located directly below microvesicles, consequently tethering these microvesicles to the surface. Despite the strong plausibility of physically restricting microvesicles, tetherin is a multifunctional protein and could also regulate MDMVs by other mechanisms crucial to microvesicle release, such as by cytoskeleton and protein scaffolding organization,^{37,83,84} lipid raft arrangement,^{85,86} or nuclear factor kappa light-chain enhancer of activated B cells activation.^{87,88}

Furthermore, it is also important to note microvesicle formation is influenced by multiple mechanisms, including lipid rearrangement,⁸⁹ actin and cytoskeleton organization,^{83,90} cytosolic calcium concentrations,⁹¹ and recruitment of cellular proteins.⁹² Because of the complex interplay of these multiple factors contributing to microvesicle regulation, the exact mechanisms tetherin uses to regulate microvesicles, and its overall impact could be context dependent. Further research is necessary to fully elucidate the mechanism by which tetherin regulates MDMVs and its specific impact in different diseases and situations.

Although MDMVs' contribution to inflammation has been well established throughout the literature, little is known about their regulation or role during HIV infection. Our findings describe a novel mechanism of MDMV restriction by the membrane protein tetherin. In HIV clinical samples, decreased tetherin expression on monocytes correlated with increased circulating MDMVs, and a murine knockout tetherin demonstrated increased circulating MDMVs and increased bleeding cessation. Furthermore, our research revealed that exposure to the viral protein Tat could be a probable mechanism for the decreased tetherin and increased circulating TF+ MDMVs observed in HIV-infected individuals. Collectively, this work builds a strong foundation to further investigate a novel mechanism for MDMV regulation, which might be expanded to all microvesicle populations. Thus, targeting tetherin could lead to new treatments for many inflammatory diseases

related to microvesicles, both in the HIV-infected and general populations.

ARTICLE INFORMATION

Received January 21, 2020; accepted June 11, 2020.

Affiliations

From the Department of Microbiology & Immunology, University of Rochester Medical Center, Rochester, NY (E.A.W., M.V.S., J.W.J., S.S., S.B.M.); Department of Basic and Clinical Sciences, Albany College of Pharmacy and Health Sciences, Rochester, NY (V.B.S.); and Aab Cardiovascular Research Institute, University of Rochester Medical Center, Rochester, NY (S.K.T., C.N.M.).

Acknowledgments

The authors thank Karen Bentley of the URMIC Electron Microscopy Core Shared Resource Lab for work in processing samples and capturing images. The authors also thank Dr Elaine Smolock, Dr Dorota Piekna-Przybylska, Sydney Simpson, Jacob Botros-Greenlee, and Edward Sombrano for helpful discussions; and the URMIC Infectious Diseases Clinic and Rochester Victory Alliance, especially Catherine Bunce, for help in acquiring donor blood samples. The authors thank the University of Rochester Center for AIDS Research for their support; and, finally, Matthew Cochran and URMIC Flow Cytometry Core for training and facilities.

Sources of Funding

The authors acknowledge funding for this work from the U.S. National Institutes of Health (R01 HL128155, R01 HL123346, R01 NS066801 and T32 AI049815) and also the University of Rochester Center for AIDS Research (UR-CFAR; P30 AI078498) for their support of core facilities.

Disclosures

None.

Supplementary Materials

Figures S1–S9

REFERENCES

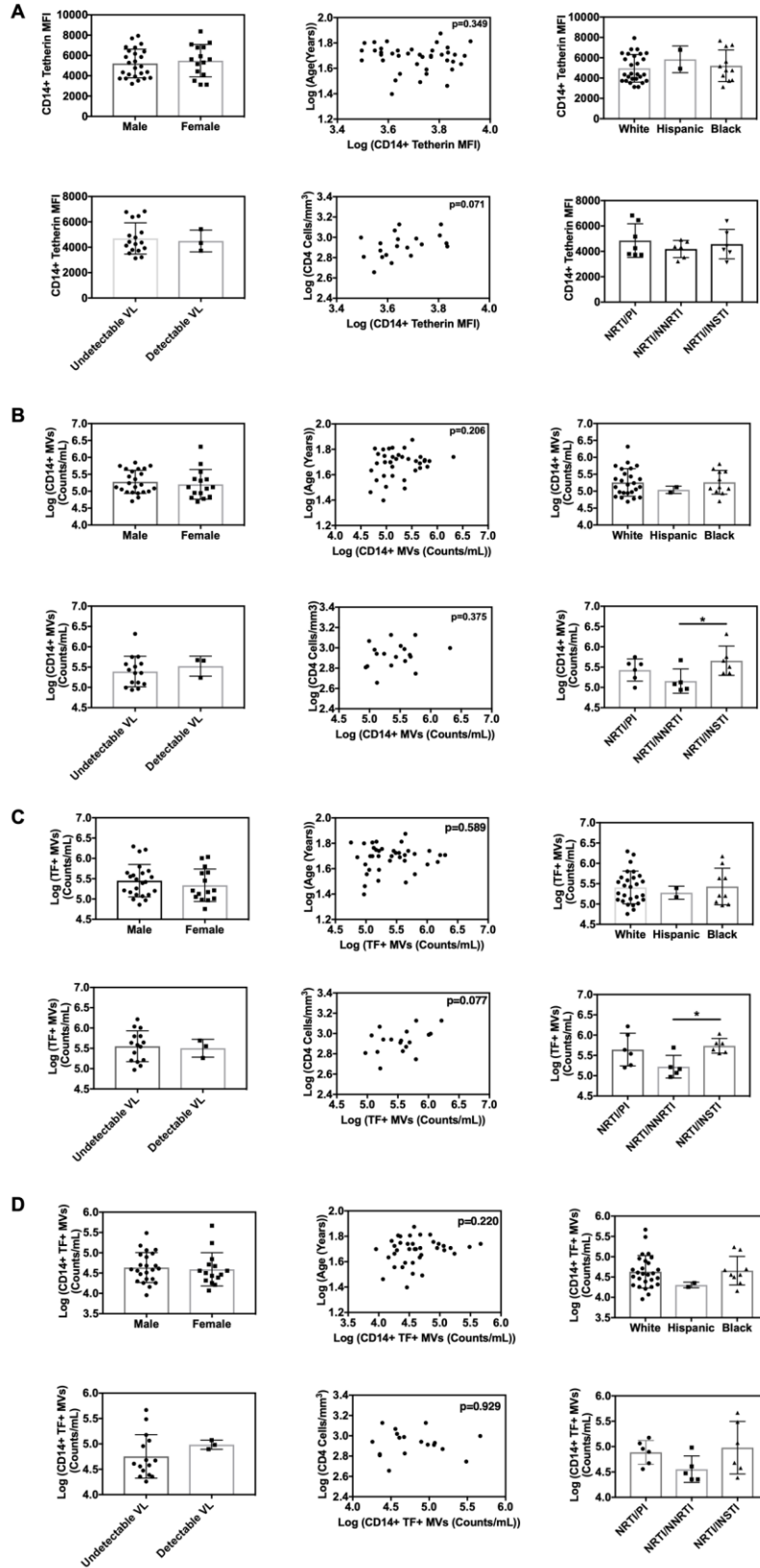
- Guaraldi G, Orlando G, Zona S, Menozzi M, Carli F, Garlassi E, Berti A, Rossi E, Roverato A, Palella F. Premature age-related comorbidities among HIV-infected persons compared with the general population. *Clin Infect Dis*. 2011;53:1120–1126.
- Saylor D, Dickens AM, Sacktor N, Haughey N, Slusher B, Pletnikov M, Mankowski JL, Brown A, Volsky DJ, McArthur JC. HIV-associated neurocognitive disorder—pathogenesis and prospects for treatment. *Nat Rev Neurol*. 2016;12:234–248.
- Schouten J, Wit FW, Stolte IG, Kootstra NA, van der Valk M, Geerlings SE, Prins M, Reiss P; AGEHIV Cohort Study Group. Cross-sectional comparison of the prevalence of age-associated comorbidities and their risk factors between hiv-infected and uninfected individuals: the AGEHIV cohort study. *Clin Infect Dis*. 2014;59:1787–1797.
- Beltrán LM, Muñoz Hernández R, de Pablo Bernal RS, García Morillo JS, Egido J, Noval ML, Ferrando-Martinez S, Blanco-Colio LM, Genebat M, Villar JR, et al. Reduced sTWEAK and increased sCD163 levels in HIV-infected patients: modulation by antiretroviral treatment, HIV replication and HCV co-infection. *PLoS One*. 2014;9:e90541.
- Hattab S, Guiguet M, Carcelain G, Fourati S, Guihot A, Autran B, Caby F, Marcelin AG, Costagliola D, Katlama C. Soluble biomarkers of immune activation and inflammation in HIV infection: impact of 2 years of effective first-line combination antiretroviral therapy. *HIV Med*. 2015;16:553–562.
- Longenecker CT, Jiang Y, Orringer CE, Gilkeson RC, Debanne S, Funderburg NT, Lederman MM, Storer N, Labbato DE, McComsey GA. Soluble CD14 is independently associated with coronary calcification and extent of subclinical vascular disease in treated HIV infection. *AIDS*. 2014;28:969–977.
- Castley A, Williams L, James I, Guelfi G, Berry C, Nolan D. Plasma CXCL10, sCD163 and sCD14 levels have distinct associations with antiretroviral treatment and cardiovascular disease risk factors. *PLoS One*. 2016;11:e0158169.
- Burdo TH, Weiffenbach A, Woods SP, Letendre S, Ellis RJ, Williams KC. Elevated sCD163 in plasma but not cerebrospinal fluid is a marker of neurocognitive impairment in HIV infection. *AIDS*. 2013;27:1387–1395.
- McGuire JL, Gill AJ, Douglas SD, Kolson DL; CNS HIV Anti-Retroviral Therapy Effects Research (CHARTER) group. Central and peripheral markers of neurodegeneration and monocyte activation in HIV-associated neurocognitive disorders. *J Neurovirol*. 2015;21:439–448.
- Sandler NG, Wand H, Roque A, Law M, Nason MC, Nixon DE, Pedersen C, Ruxrungtham K, Lewin SR, Emery S, et al. Plasma levels of soluble CD14 independently predict mortality in HIV infection. *J Infect Dis*. 2011;203:780–790.
- Williams B, Livak B, Bahk M, Keating SM, Adeyemi OM. Short communication: SCD14 and SCD163 levels are correlated with VACS index scores: initial data from the blunted immune recovery in CORE patients with HIV (BIRCH) cohort. *AIDS Res Hum Retroviruses*. 2016;32:144–147.
- Knudsen TB, Ertner G, Petersen J, Møller HJ, Moestrup SK, Eugen-Olsen J, Kronborg G, Benfield T. Plasma soluble CD163 level independently predicts all-cause mortality in HIV-1-infected individuals. *J Infect Dis*. 2016;214:1198–1204.
- Del Conde I, Shrimpton CN, Thiagarajan P, López JA. Tissue-factor-bearing microvesicles arise from lipid rafts and fuse with activated platelets to initiate coagulation. *Blood*. 2005;106:1604–1611.
- Barteneva NS, Faslser-Kan E, Bernimoulin M, Stern JN, Ponomarev ED, Duckett L, Vorobjev IA. Circulating microparticles: square the circle. *BMC Cell Biol*. 2013;14:23.
- Marcoux G, Duchez AC, Cloutier N, Provost P, Nigrovic PA, Boilard E. Revealing the diversity of extracellular vesicles using high-dimensional flow cytometry analyses. *Sci Rep*. 2016;6:35928.
- Mack M, Kleinschmidt A, Brühl H, Klier C, Nelson PJ, Cihak J, Plachý J, Stangassinger M, Erfle V, Schlöndorff D. Transfer of the chemokine receptor ccr5 between cells by membrane-derived microparticles: a mechanism for cellular human immunodeficiency virus 1 infection. *Nat Med*. 2000;6:769–775.
- Sahler J, Woeller C, Spinelli S, Blumberg N, Phipps R. A novel method for overexpression of peroxisome proliferator-activated receptor-γ in megakaryocyte and platelet microparticles achieves transcellular signaling. *J Thromb Haemost*. 2012;10:2563–2572.
- Barry OP, Pratico D, Lawson JA, FitzGerald GA. Transcellular activation of platelets and endothelial cells by bioactive lipids in platelet microparticles. *J Clin Invest*. 1997;99:2118–2127.
- Ratajczak J, Miekus K, Kucia M, Zhang H, Reza R, Dvorak P, Ratajczak MZ. Embryonic stem cell-derived microvesicles reprogram hematopoietic progenitors: evidence for horizontal transfer of mRNA and protein delivery. *Leukemia*. 2006;20:847–856.
- Dubreau LH, Duchez AC, Cloutier N, Soulet D, Martin N, Bollinger J, Paré A, Rousseau M, Naika GS, Lévesque T, et al. Platelets release mitochondria serving as substrate for bactericidal group IIA-secreted phospholipase A2 to promote inflammation. *Blood*. 2014;124:2173–2183.
- Lai FW, Lichty BD, Bowdish DM. Microvesicles: ubiquitous contributors to infection and immunity. *J Leukoc Biol*. 2015;97:237–245.
- Wen B, Combes V, Bonhoure A, Weksler BB, Couraud PO, Grau GE. Endotoxin-induced monocytic microparticles have contrasting effects on endothelial inflammatory responses. *PLoS One*. 2014;9:e91597.
- Wang JG, Williams JC, Davis BK, Jacobson K, Doerschuk CM, Ting JP, Mackman N. Monocytic microparticles activate endothelial cells in an IL-1β-dependent manner. *Blood*. 2011;118:2366–2374.
- Khaspekova SG, Antonova OA, Shustova ON, Yakushkin VV, Golubeva NV, Titavaeva EV, Dobrovolsky AB, Mazurov AV. Activity of tissue factor in microparticles produced in vitro by endothelial cells, monocytes, granulocytes, and platelets. *Biochemistry (Mosc)*. 2016;81:114–121.
- Satta N, Toti F, Feugeas O, Bohbot A, Dachary-Prigent J, Eschwège V, Hedman H, Freyssinet JM. Monocyte vesiculation is a possible mechanism for dissemination of membrane-associated procoagulant activities and adhesion molecules after stimulation by lipopolysaccharide. *J Immunol*. 1994;153:3245–3255.
- Herring JM, McMichael MA, Smith SA. Microparticles in health and disease. *J Vet Intern Med*. 2013;27:1020–1033.
- Kornek M, Schuppan D. Microparticles: modulators and biomarkers of liver disease. *J Hepatol*. 2012;57:1144–1146.
- Diamant M, Nieuwland R, Pablo RF, Sturk A, Smit JW, Radder JK. Elevated numbers of tissue-factor exposing microparticles correlate

- with components of the metabolic syndrome in uncomplicated type 2 diabetes mellitus. *Circulation*. 2002;106:2442–2447.
29. Daniel L, Fakhouri F, Joly D, Mouthon L, Nusbaum P, Grunfeld JP, Schifferli J, Guillemin L, Lesavre P, Halbwachs-Mecarelli L. Increase of circulating neutrophil and platelet microparticles during acute vasculitis and hemodialysis. *Kidney Int*. 2006;69:1416–1423.
 30. Liu Y, He Z, Zhang Y, Dong Z, Bi Y, Kou J, Zhou J, Shi J. Dissimilarity of increased phosphatidylserine-positive microparticles and associated coagulation activation in acute coronary syndromes. *Coron Artery Dis*. 2016;27:365–375.
 31. Sarlon-Bartoli G, Bennis Y, Lacroix R, Piercecchi-Marti MD, Bartoli MA, Arnaud L, Mancini J, Boudes A, Sarlon E, Thevenin B, et al. Plasmatic level of leukocyte-derived microparticles is associated with unstable plaque in asymptomatic patients with high-grade carotid stenosis. *J Am Coll Cardiol*. 2013;62:1436–1441.
 32. Price JC, Thio CL. Liver disease in the hiv-infected individual. *Clin Gastroenterol Hepatol*. 2010;8:1002–1012.
 33. Hijmans JG, Stockelman KA, Garcia V, Levy MV, Brewster LM, Bammert TD, Greiner JJ, Stauffer BL, Connick E, DeSouza CA. Circulating microparticles are elevated in treated HIV -1 infection and are deleterious to endothelial cell function. *J Am Heart Assoc*. 2019;8:e011134. DOI: 10.1161/JAHA.118.011134.
 34. Neil SJ, Zang T, Bieniasz PD. Tetherin inhibits retrovirus release and is antagonized by HIV-1 Vpu. *Nature*. 2008;451:425–430.
 35. Takahashi T, Suzuki T. Function of membrane rafts in viral lifecycles and host cellular response. *Biochem Res Int*. 2011;2011:245090.
 36. Venkatesh S, Bieniasz PD. Mechanism of HIV-1 virion entrapment by tetherin. *PLoS Pathog*. 2013;9:e1003483.
 37. Rollason R, Korolchuk V, Hamilton C, Jepson M, Banting G. A CD317/tetherin-RIICH2 complex plays a critical role in the organization of the subapical actin cytoskeleton in polarized epithelial cells. *J Cell Biol*. 2009;184:721–736.
 38. Edgar JR, Manna PT, Nishimura S, Banting G, Robinson MS. Tetherin is an exosomal tether. *Elife*. 2016;5:e17180.
 39. Margolis L, Sadvovsky Y. The biology of extracellular vesicles: the known unknowns. *PLoS Biol*. 2019;17:e3000363.
 40. Connor R, Jones LD, Qiu X, Thakar J, Maggirwar SB. Frontline science: c-Myc regulates P-selectin glycoprotein ligand-1 expression in monocytes during HIV-1 infection. *J Leukoc Biol*. 2017;102:953–964.
 41. Liberatore RA, Bieniasz PD. Tetherin is a key effector of the antiretroviral activity of type I interferon in vitro and in vivo. *Proc Natl Acad Sci USA*. 2011;108:18097–18101.
 42. Badou A, Bennasser Y, Moreau M, Leclerc C, Benkirane M, Bahraoui E. Tat protein of human immunodeficiency virus type 1 induces interleukin-10 in human peripheral blood monocytes: implication of protein kinase C-dependent pathway. *J Virol*. 2000;74:10551–10562.
 43. Park J, Ryu J, Kim KA, Lee HJ, Bahn JH, Han K, Choi EY, Lee KS, Kwon HY, Choi SY. Mutational analysis of a human immunodeficiency virus type 1 Tat protein transduction domain which is required for delivery of an exogenous protein into mammalian cells. *J Gen Virol*. 2002;83:1173–1181.
 44. Brailoiu E, Deliu E, Sporici RA, Benamar K, Brailoiu GC. HIV-1-Tat excites cardiac parasympathetic neurons of nucleus ambiguus and triggers prolonged bradycardia in conscious rats. *Am J Physiol Regul Integr Comp Physiol*. 2014;306:R814–R822.
 45. Viswanathan K, Smith MS, Malouli D, Mansouri M, Nelson JA, Früh K. BST2/tetherin enhances entry of human cytomegalovirus. *PLoS Pathog*. 2011;7:e1002332.
 46. Kizilyer A, Singh MV, Singh VB, Suwunnakorn S, Palis J, Maggirwar SB. Inhibition of tropomyosin receptor kinase a signaling negatively regulates megakaryopoiesis and induces thrombopoiesis. *Sci Rep*. 2019;9:2781.
 47. Gustin JK, Douglas JL, Bai Y, Moses AV. Ubiquitination of BST-2 protein by HIV-1 Vpu protein does not require lysine, serine, or threonine residues within the BST-2 cytoplasmic domain. *J Biol Chem*. 2012;287:14837–14850.
 48. Mansouri M, Viswanathan K, Douglas JL, Hines J, Gustin J, Moses AV, Früh K. Molecular mechanism of BST2/tetherin downregulation by K5/MIR2 of Kaposi's sarcoma-associated herpesvirus. *J Virol*. 2009;83:9672–9681.
 49. Kutner RH, Zhang XY, Reiser J. Production, concentration and titration of pseudotyped HIV-1-based lentiviral vectors. *Nat Protoc*. 2009;4:495–505.
 50. Sommer JM, Smith PH, Parthasarathy S, Isaacs J, Vijay S, Kieran J, Powell SK, McClelland A, Wright JF. Quantification of adeno-associated virus particles and empty capsids by optical density measurement. *Mol Ther*. 2003;7:122–128.
 51. Singh VB, Wooten AK, Jackson JW, Maggirwar SB, Kieba M. Investigating the role of ankyrin-rich membrane spanning protein in human immunodeficiency virus type-1 Tat-induced microglia activation. *J Neurovirol*. 2015;21:186–198.
 52. Singh VB, Singh MV, Gorantla S, Poluektova LY, Maggirwar SB. Smoothed agonist reduces human immunodeficiency virus type-1-induced blood-brain barrier breakdown in humanized mice. *Sci Rep*. 2016;6:26876.
 53. Davidson DC, Hirschman MP, Sun A, Singh MV, Kasischke K, Maggirwar SB. Excess soluble CD40L contributes to blood brain barrier permeability in vivo: implications for HIV-associated neurocognitive disorders. *PLoS One*. 2012;7:e51793.
 54. Mayne E, Funderburg NT, Sieg SF, Asaad R, Kalinowska M, Rodriguez B, Schmaier AH, Stevens W, Lederman MM. Increased platelet and microparticle activation in HIV infection: upregulation of P-selectin and tissue factor expression. *J Acquir Immune Defic Syndr*. 2012;59:340–346.
 55. Kaneko T, Fujii S, Matsumoto A, Goto D, Makita N, Hamada J, Moriuchi T, Kitabatake A. Induction of tissue factor expression in endothelial cells by basic fibroblast growth factor and its modulation by fenofibric acid. *Thromb J*. 2003;1:6.
 56. Wu Y, Deng W, Klinke DJ. Exosomes: improved methods to characterize their morphology, RNA content, and surface protein biomarkers. *Analyst*. 2015;140:6631–6642.
 57. Wolf JM, Espadas-Moreno J, Luque-Garcia JL, Casadevall A. Interaction of *Cryptococcus neoformans* extracellular vesicles with the cell wall. *Eukaryot Cell*. 2014;13:1484–1493.
 58. Dubé M, Bego MG, Paquay C, Cohen É. Modulation of HIV-1-host interaction: role of the Vpu accessory protein. *Retrovirology*. 2010;7:114.
 59. McElrath MJ, Steinman RM, Cohn ZA. Latent HIV-1 infection in enriched populations of blood monocytes and T cells from seropositive patients. *J Clin Invest*. 1991;87:27–30.
 60. Massanella M, Bakeman W, Sithinamsuwan P, Fletcher JLK, Chomchey N, Tipsuk S, Chalermchai T, Routy JP, Ananworanich J, Valcour VG, et al. Infrequent hiv infection of circulating monocytes during antiretroviral therapy. *J Virol*. 2019;94.
 61. Xiao H, Neuveut C, Tiffany HL, Benkirane M, Rich EA, Murphy PM, Jeang KT. Selective CXCR4 antagonism by Tat: implications for in vivo expansion of coreceptor use by HIV-1. *Proc Natl Acad Sci U S A*. 2000;97:11466–11471.
 62. Mediouni S, Darque A, Baillat G, Ravaux I, Dhiver C, Tissot-Dupont H, Mokhtari M, Moreau H, Tamalet C, Brunet C, et al. Antiretroviral therapy does not block the secretion of the human immunodeficiency virus tat protein. *Infect Disord Drug Targets*. 2012;12:81–86.
 63. Clark E, Nava B, Caputi M. Tat is a multifunctional viral protein that modulates cellular gene expression and functions. *Oncotarget*. 2017;8:27569–27581.
 64. Gross PL, Furie BC, Merrill-Skoloff G, Chou J, Furie B. Leukocyte-versus microparticle-mediated tissue factor transfer during arteriolar thrombus development. *J Leukoc Biol*. 2005;78:1318–1326.
 65. Chou J, Mackman N, Merrill-Skoloff G, Pedersen B, Furie BC, Furie B. Hematopoietic cell-derived microparticle tissue factor contributes to fibrin formation during thrombus propagation. *Blood*. 2004;104:3190–3197.
 66. Funderburg NT, Mayne E, Sieg SF, Asaad R, Jiang W, Kalinowska M, Luciano AA, Stevens W, Rodriguez B, Brenchley JM, et al. Increased tissue factor expression on circulating monocytes in chronic HIV infection: relationship to in vivo coagulation and immune activation. *Blood*. 2010;115:161–167.
 67. Paulaitis ME, Agarwal K, Nana-Sinkam SP. Dynamic scaling of exosome sizes. *Langmuir*. 2018.
 68. Hughes M, Hayward CP, Warkentin TE, Horsewood P, Chorneyko KA, Kelton JG. Morphological analysis of microparticle generation in heparin-induced thrombocytopenia. *Blood*. 2000;96:188–194.
 69. Ponomareva AA, Nevzorova TA, Mordakhanova ER, Andrianova IA, Rauova L, Litvinov RI, Weisel JW. Intracellular origin and ultrastructure of platelet-derived microparticles. *J Thromb Haemost*. 2017;15:1655–1667.
 70. Mackman N. The role of tissue factor and factor VIIa in hemostasis. *Anesth Analg*. 2009;108:1447–1452.

71. Currier JS, Taylor A, Boyd F, Dezil CM, Kawabata H, Burtcel B, Maa JF, Hodder S. Coronary heart disease in HIV-infected individuals. *J Acquir Immune Defic Syndr*. 2003;33:506–512.
72. Freiberg MS, Chang CC, Kuller LH, Skanderson M, Lowy E, Kraemer KL, Butt AA, Bidwell Goetz M, Leaf D, Oursler KA, et al. HIV infection and the risk of acute myocardial infarction. *JAMA Intern Med*. 2013;173:614–622.
73. Johnson TP, Patel K, Johnson KR, Maric D, Calabresi PA, Hasbun R, Nath A. Induction of IL-17 and nonclassical T-cell activation by HIV-Tat protein. *Proc Natl Acad Sci U S A*. 2013;110:13588–13593.
74. Dhamija N, Choudhary D, Ladha JS, Pillai B, Mitra D. Tat predominantly associates with host promoter elements in HIV-1-infected T-cells—regulatory basis of transcriptional repression of c-Rel. *FEBS J*. 2015;282:595–610.
75. Kambara H, Gunawardane L, Zebrowski E, Kostadinova L, Jobava R, Krokowski D, Hatzoglou M, Anthony DD, Valadkhan S. Regulation of interferon-stimulated gene BST2 by a lncRNA transcribed from a shared bidirectional promoter. *Front Immunol*. 2014;5:676.
76. Planès R, Ben Haij N, Leghmari K, Serrero M, BenMohamed L, Bahaoui E. HIV-1 Tat protein activates both the MyD88 and TRIF pathways to induce tumor necrosis factor alpha and interleukin-10 in human monocytes. *J Virol*. 2016;90:5886–5898.
77. Jones PH, Okeoma CM. Phosphatidylinositol 3-kinase is involved in Toll-like receptor 4-mediated BST-2/tetherin regulation. *Cell Signal*. 2013;25:2752–2761.
78. Blondeau C, Pelchen-Matthews A, Mlcochova P, Marsh M, Milne RS, Towers GJ. Tetherin restricts herpes simplex virus 1 and is antagonized by glycoprotein M. *J Virol*. 2013;87:13124–13133.
79. Kaletsky RL, Francica JR, Agrawal-Gamse C, Bates P. Tetherin-mediated restriction of filovirus budding is antagonized by the Ebola glycoprotein. *Proc Natl Acad Sci U S A*. 2009;106:2886–2891.
80. Pan XB, Han JC, Cong X, Wei L. BST2/tetherin inhibits dengue virus release from human hepatoma cells. *PLoS One*. 2012;7:e51033.
81. Perez-Caballero D, Zang T, Ebrahimi A, McNatt MW, Gregory DA, Johnson MC, Bieniasz PD. Tetherin inhibits HIV-1 release by directly tethering virions to cells. *Cell*. 2009;139:499–511.
82. Kupzig S, Korolchuk V, Rollason R, Sugden A, Wilde A, Banting G. Bst-2/HM1.24 is a raft-associated apical membrane protein with an unusual topology. *Traffic*. 2003;4:694–709.
83. Muralidharan-Chari V, Clancy J, Plou C, Romao M, Chavrier P, Raposo G, D'Souza-Schorey C. Arf6-regulated shedding of tumor cell-derived plasma membrane microvesicles. *Curr Biol*. 2009;19:1875–1885.
84. Miyakawa K, Ryo A, Murakami T, Ohba K, Yamaoka S, Fukuda M, Guatelli J, Yamamoto N. BCA2/Rabring7 promotes tetherin-dependent HIV-1 restriction. *PLoS Pathog*. 2009;5:e1000700.
85. Billcliff PG, Rollason R, Prior I, Owen DM, Gaus K, Banting G. CD317/tetherin is an organiser of membrane microdomains. *J Cell Sci*. 2013;126:1553–1564.
86. Wei H, Malcor JM, Harper MT. Lipid rafts are essential for release of phosphatidylserine-exposing extracellular vesicles from platelets. *Sci Rep*. 2018;8:9987.
87. Johnson BL, Goetzman HS, Prakash PS, Caldwell CC. Mechanisms underlying mouse TNF- α stimulated neutrophil derived microparticle generation. *Biochem Biophys Res Commun*. 2013;437:591–596.
88. Galão RP, Le Tortorec A, Pickering S, Kueck T, Neil SJ. Innate sensing of HIV-1 assembly by tetherin induces NF κ B-dependent proinflammatory responses. *Cell Host Microbe*. 2012;12:633–644.
89. Morel O, Jesel L, Freyssinet JM, Toti F. Cellular mechanisms underlying the formation of circulating microparticles. *Arterioscler Thromb Vasc Biol*. 2011;31:15–26.
90. Li B, Antonyak MA, Zhang J, Cerione RA. RhoA triggers a specific signaling pathway that generates transforming microvesicles in cancer cells. *Oncogene*. 2012;31:4740–4749.
91. Crawford S, Diamond D, Brustolon L, Penarreta R. Effect of increased extracellular Ca on microvesicle production and tumor spheroid formation. *Cancer Microenviron*. 2010;4:93–103.
92. Nabhan JF, Hu R, Oh RS, Cohen SN, Lu Q. Formation and release of arrestin domain-containing protein 1-mediated microvesicles (ARMMs) at plasma membrane by recruitment of TSG101 protein. *Proc Natl Acad Sci U S A*. 2012;109:4146–4151.

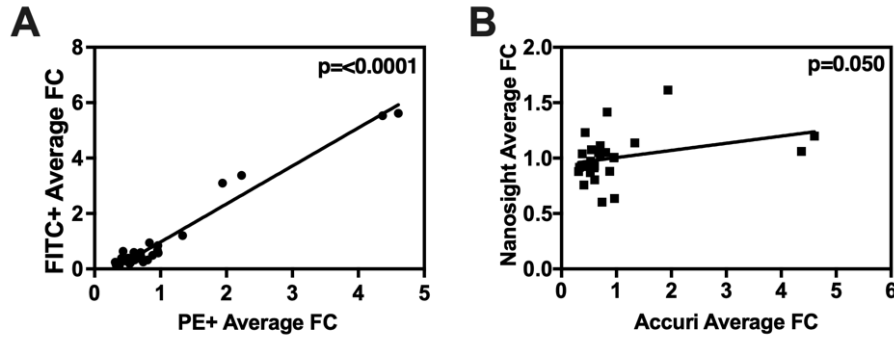
SUPPLEMENTAL MATERIAL

Figure S1. Donor characteristics in relation to CD14+ tetherin, CD14+ MVs, tissue factor+ (TF+) MVs, and CD14+TF+ microvesicles (MV) levels.



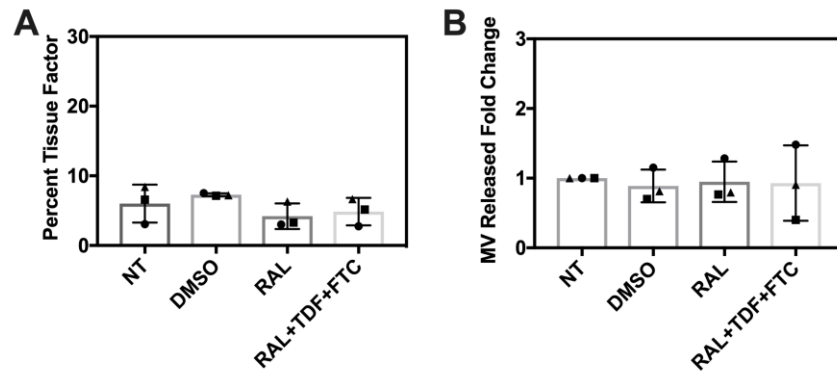
(A-D) Sex, age, and ethnicity for all donors, and for HIV+ donors viral loads (VL), CD4+ T cell count, and type of treatment (including combinations of nucleoside reverse transcriptase inhibitors (NRTIs) with protease inhibitors (PIs) or non-nucleoside reverse transcriptase inhibitors (NNRTIs) or integrase strand transfer inhibitors (INSTIs)), were compared in CD14+ tetherin expression (A), circulating CD14+ MV (B), circulating TF+ MV (C), and circulating CD14+ TF+ MV(D) levels. Comparing between sexes differences for CD14+ and CD14+ TF+ MVs, the Mann-Whitney test was used; comparing differences between sexes for tetherin and TF+ MVs, unpaired t test was used. To evaluate CD14+ MVs, TF+ MVs and CD14+ TF+ MVs in correlation to age, Pearson correlation analysis was used. To evaluate tetherin in correlation to age, Spearman correlation analysis was used. For all comparisons between ethnicity and types of treatment, a one-way ANOVA test with Tukey's multiple comparisons was performed. For tetherin expression, TF+ MVs, and CD14+ TF+ MVs comparing different viral loads, unpaired t test was used. For CD14+ MVs in comparing viral load, Mann-Whitney test was used. To evaluate all CD4 cells counts in correlation to either tetherin or MV levels, Pearson correlation analysis was used.

Figure S2. Validation of Accuri quantification of CD14+ MVs.



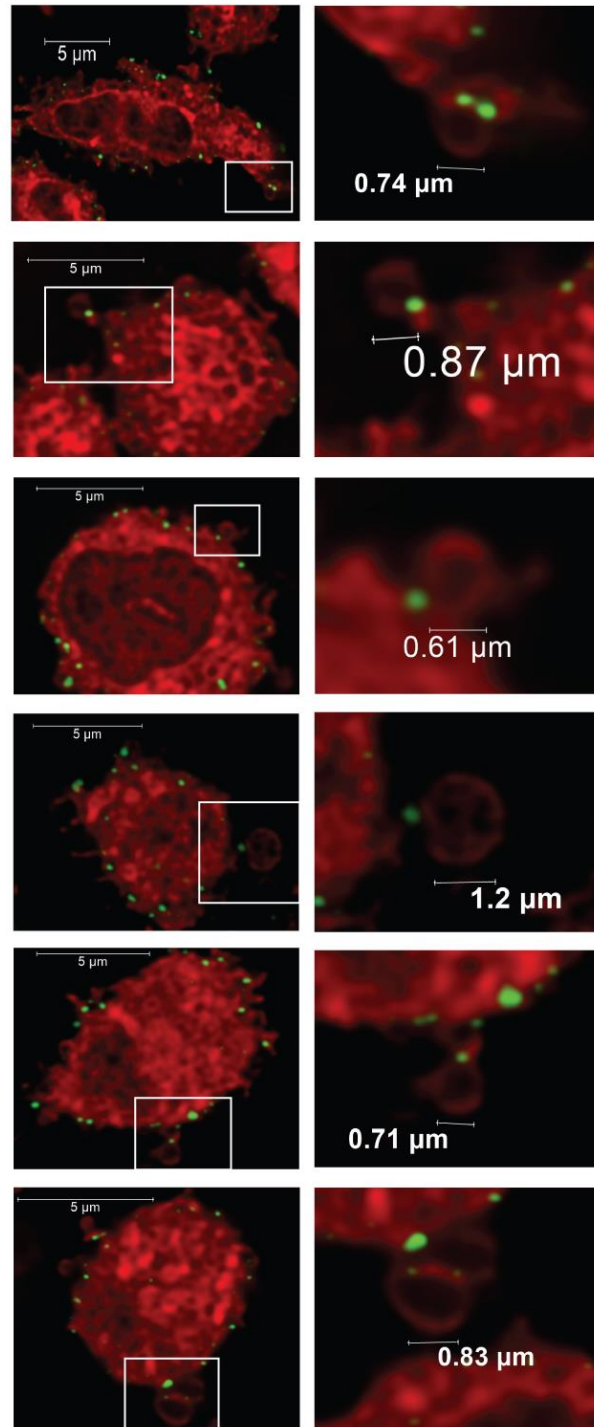
(A) Plasma was collected from consented donors and was spun to remove platelets and cell debris. Each sample was stained with two different antibodies, both against CD14, but with different epitopes and fluorophores. The fold change (FC) over the average was taken for each donor and correlated against the different antibodies. Spearman correlation analysis was performed to evaluate the correlation between the fold change of MVs using the FITC CD14+ antibody and the PE CD14+ antibody. (N=29). (B) Plasma from the same donors were stained CD14 with FITC and analyzed by NS300 and NTA or stained for CD14 conjugated to PE followed by quantification on the BD Accuri C6. Spearman correlation analysis was performed to evaluate the correlation between MVs quantified by the NS300 and MVs quantified by the BD Accuri C6. (N=28).

Figure S3. Integrase inhibitor effect on monocyte tissue factor (TF) expression and microvesicle (MV) release.



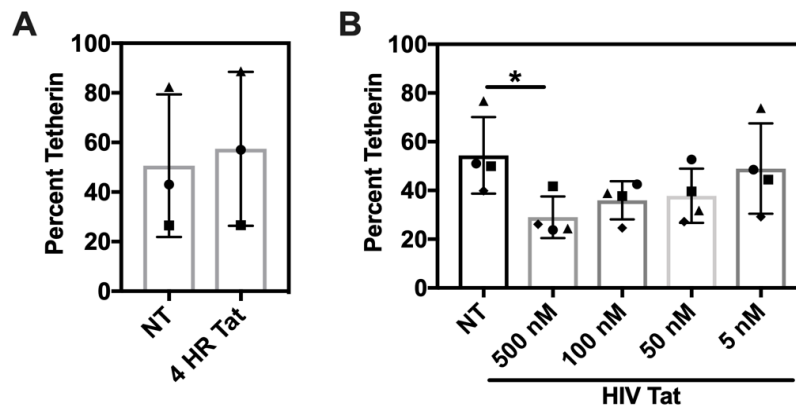
Primary monocytes were isolated from HIV- donors and exposed for 18-24 hours to the integrase inhibitor raltegravir (RAL, 5 μ M) alone or in combination with common nucleoside reverse transcriptase inhibitors tenofovir disoproxil fumarate (TDF, 5 μ M) or emtricitabine (FTC, 5 μ M). Dimethyl sulfoxide (DMSO) served as a vehicle control. (A) Monocytes were then fixed and stained. TF expression was quantified by flow cytometry. (B) Media was then collected, centrifuged to remove cell debris, and analyzed for MV content using NTA. (N=3 biological replicates averaged from 1-2 technical replicates).

Figure S4. Super resolution microscopy of tetherin on the surface of monocytes.



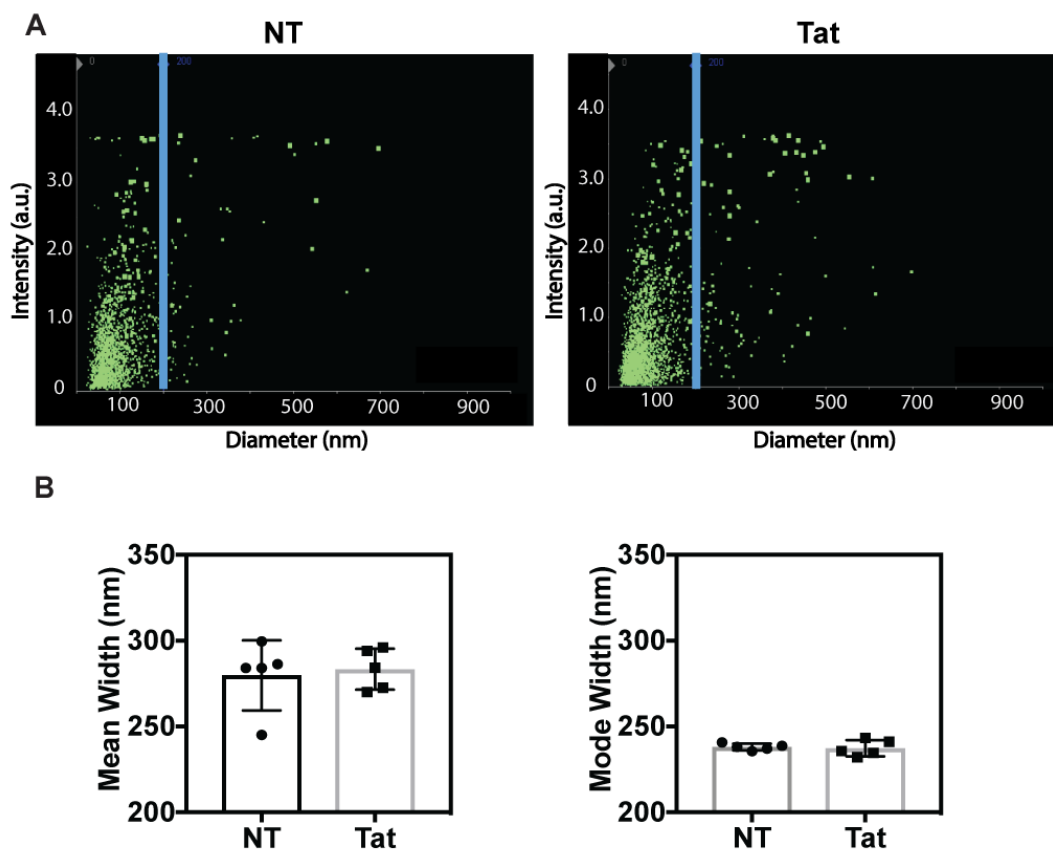
Primary monocytes were isolated from HIV- donors and fixed in PFA. Cells were then labeled for tetherin (green) and Cell Mask Red was used to mark the cell membrane (red). White boxes inset in images on left represent areas shown enlarged on right.

Figure S5. Tetherin expression on Tat-treated monocytes.



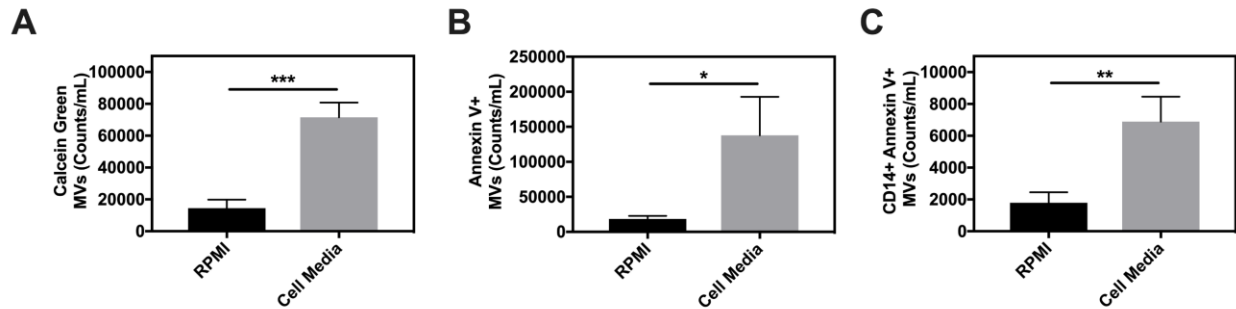
(A) Primary monocytes were exposed to Tat (500 nM) for 4 hours (4 HR Tat). Quantification of tetherin expression on cells was measured by flow cytometry (N=3 biological replicates averaged from 2-3 technical replicates) and compared using a paired t test. (B) Primary monocytes treated Tat for 18 hours and fixed. Tetherin expression was quantified by flow cytometry and expression between concentrations was compared using a one-way ANOVA test with Dunnett's multiple comparisons test. (N=4 biological replicates averaged from 2-3 technical replicates).

Figure S6. Size analysis of *in vitro* particles from Tat-treated monocytes.



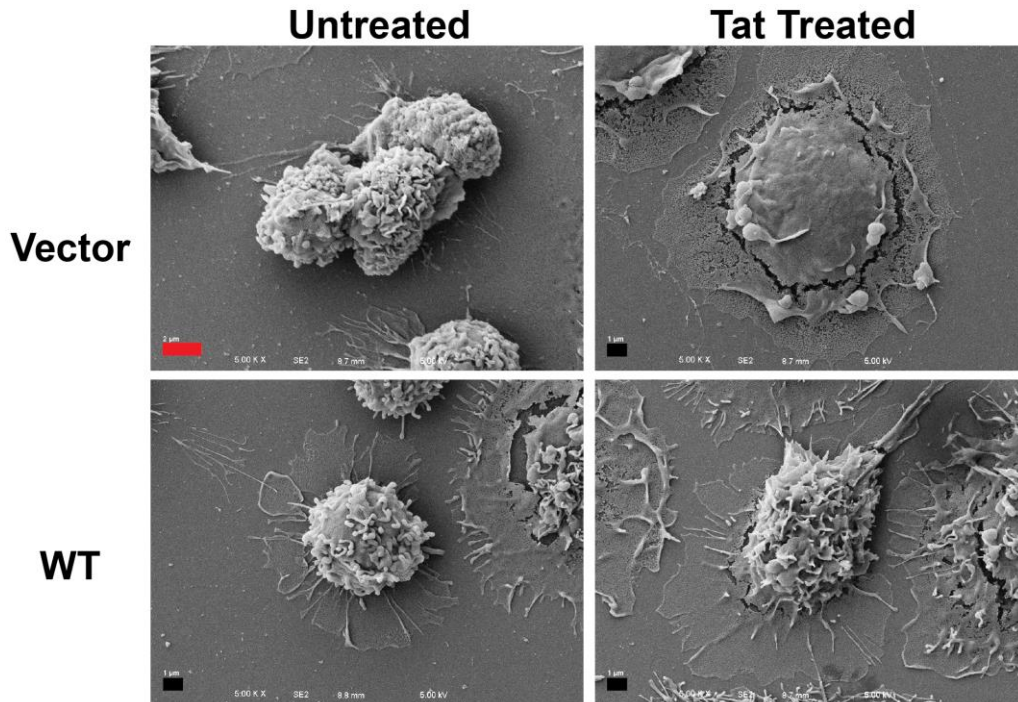
(A) Primary monocytes treated with the HIV Tat (500 nM) and media was collected for particle analysis using the NS500 and NanoSight Tracking Analysis. Represented plots of particles for non-treated (NT) and Tat-treated (Tat) are displayed with the blue line delineating the 200 nm size. (B) The mean and mode of particles greater than 200 nm was calculated for each sample and compared using paired t test.

Figure S7. *In vitro* microvesicle (MV) analysis.



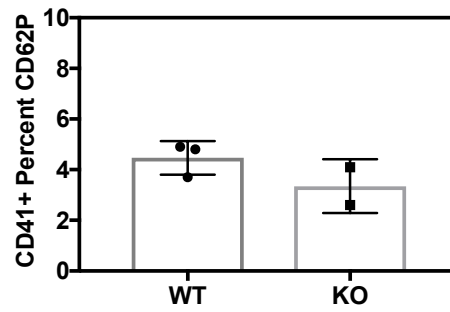
To characterize MVs released by primary monocytes in cell culture, cells were harvested from a healthy donor and incubated in media overnight. The media was then centrifuged to remove cells and stained with calcein green to observe if particles were membrane bound. Additionally, MVs were isolated by high speed centrifugation, resuspending in Annexin V binding buffer, and stained for Annexin V and CD14. All MVs were quantified using flow cytometry. Media isolated from cells contained significantly higher amounts of MVs than that observed in media alone. (N=3 technical replicates). All experiments were compared using an unpaired t test.

Figure S8. SEM of monocytes overexpressing tetherin.



Primary monocytes were isolated and infected with lentiviruses to over express tetherin. The vectors used were empty vector (Vector) or wild-type tetherin (WT). Transfected monocytes were either left untreated or treated with the viral protein Tat (100nM) for 1 hour followed by fixation and preparation for scanning electron microscopy (SEM) as outlined in the method section. In left corner of image, black bars denote 1μM and red bars denote 2μM.

Figure S9. Platelet activation in Tetherin knock-out (KO) mice.



Aged- and sex-matched wild-type (WT) and KO over the age of 8 weeks were bled retro-orbitally. Blood was then fixed and stained for CD41 to identify platelets and CD62P to mark activation. Samples were run through flow cytometry and the percent of platelets expressing CD62P was measured and compared using unpaired t test.